
ETD Archive

2013

NOS Oxygenase-Mediated Nitroalkane Catalytic Reduction: Impact on NOS Reaction

Praneeth Ivan joel Fnu
Cleveland State University

Follow this and additional works at: <https://engagedscholarship.csuohio.edu/etdarchive>

 Part of the [Chemistry Commons](#)

[How does access to this work benefit you? Let us know!](#)

Recommended Citation

Fnu, Praneeth Ivan joel, "NOS Oxygenase-Mediated Nitroalkane Catalytic Reduction: Impact on NOS Reaction" (2013). *ETD Archive*. 819.
<https://engagedscholarship.csuohio.edu/etdarchive/819>

This Thesis is brought to you for free and open access by EngagedScholarship@CSU. It has been accepted for inclusion in ETD Archive by an authorized administrator of EngagedScholarship@CSU. For more information, please contact library.es@csuohio.edu.

**NOS OXYGENASE-MEDIATED NITROALKANE CATALYTIC
REDUCTION: IMPACT ON NOS REACTION**

PRANEETH IVAN JOEL FNU

Bachelor's in Pharmacy

Manipal University

India

May, 2011

Submitted in partial fulfillment of requirements

For the degree

MASTER OF SCIENCE IN CHEMISTRY

At

CLEVELAND STATE UNIVERSITY

December 2013

We hereby approve this thesis of

Praneeth Ivan Joel FNU

Candidate for the Master of Science in Chemistry degree for the

Department of CHEMISTRY

and the Cleveland State University

College of Graduate Studies by

Thesis Chairperson, *Dr. Mekki Bayachou*

Department & Date

Thesis Committee Member, *Dr. John. F. Turner*

Department & Date

Thesis Committee Member, *Dr. Robert Wei*

Department & Date

Students Date of Defense: (12/19/2013)

NOS OXYGENASE-MEDIATED NITROALKANE CATALYTIC REDUCTION: IMPACT ON NOS REACTION

PRANEETH IVAN JOEL FNU

ABSTRACT

Organic nitroalkanes are used in many industries and for a variety of purposes. Their use is expanding and is steadily claiming new territories in our immediate environment. Some nitroalkanes, when they enter the human body, can be harmful as such or can be activated to generate reactive intermediates with known detrimental effects. P450 enzymes are known for metabolizing a variety of drugs and substances including organic nitroalkanes. Nitric oxide synthases (NOS) exhibit some similarities to P450 metalloenzymes and their potential interaction with nitroalkanes as xenobiotics is not well known. The present study investigates the effect of nitroalkanes on the catalytic reaction of NOS in light of the NOS-mediated catalytic reduction of the same nitroalkanes.

In this work, we used the recombinant oxygenase domain of inducible nitric oxide synthase (iNOSoxy) and endothelial nitric oxide synthase (eNOSoxy). We have previously shown that the oxygenase domain of nitric oxide synthases (NOSs) in thin surfactant films can exchange electrons with the underlying electrode. We show in the current work that NOS oxygenase domains act as efficient electrocatalysts for nitroalkane reductions in surfactant films on pyrolytic graphite electrodes. We monitored the NOSoxy-mediated catalytic reduction of a series of nitroalkanes using electrochemical techniques. Concomitantly, we used chemical assays such as the Griess assay to assess enzymatic activity of NOSoxys under the same conditions. Voltammograms at different concentrations of nitroalkanes and different scan rates were used to derive catalytic parameters such as catalytic efficiency, K_m and k_{cat} values for

NOSoxy-mediated catalytic reduction of nitroalkanes. Overall, we present a comparative study of the electroreduction of nitromethane, nitroethane, and nitropropane using eNOSoxy and iNOSoxy as electrocatalysts. We also compare and contrast how -and the extent to which- each nitroalkane affects the catalytic NOS reaction by iNOSoxy and eNOSoxy.

TABLE OF CONTENTS

	Page
ABSTRACT.....	iii
LIST OF FIGURES.....	vii
LIST OF SCHEMES AND TABLES.....	xi
ABBREVIATIONS.....	xii
GENERAL INTRODUCTION.....	1
PROTOCOL FOR THE EXPRESSION AND PURIFICATION OF INDUCIBLE AND ENDOTHELIAL NITRIC OXIDE SYNTHASE OXYGENASE DOMAIN.....	4

CHAPTER I

NOS OXYGENASE MEDIATED NITROALKANE ELECTROREDUCTION

1.1. Introduction.....	6
1.2. Cytochrome P450s.....	7
1.3. Nitric Oxide Synthases.....	10
1.4. Similarities between Nitric Oxide synthases and P450 enzymes.....	13

CHAPTER II

iNOSoxy AND eNOSoxy MEDIATED NITROALKANE ELECTROREDUCTION

2.1. Introduction.....	15
2.2. Electrochemical Methods and Application to the study of redox proteins.....	17
2.3 Protein immobilization method.....	19
2.3.1 Formation of covalent bonds.....	20
2.3.2 Adsorption.....	21
2.3.3 Entrapment in thin films.....	21

2.3.4	Lipid bilayered thin films	22
2.4.	Method	23
2.4.1	Materials	24
2.4.2	Fabrication and modification of working electrodes	25
2.5	Results and Discussion	27
2.5.1	Direct electron transfer to iNOSoxy in surfactant films on pyrolytic graphite and catalytic reduction of nitromethane	27
2.5.2	Electrocatalytic reduction of nitromethane catalyzed by iNOSoxy	29
2.5.3	Effect of nitromethane concentration	30
2.5.4	Effect of scan rate	33
2.5.5	Peak potentials	35
2.5.6	Comparison of the electroreduction of different Nitroalkanes on iNOSoxy In ddab surfactant films	36
2.5.6.1	Effect of the nitroalkane concentration	36
2.5.6.2	Catalytic efficiency versus scan rate	38
2.5.7	Redox properties of eNOSoxy in surfactant films on PG electrodes and eNOSoxy-mediated catalytic reduction of nitromethane	39
2.5.7.1	Electrocatalytic reduction of nitromethane on eNOSoxy/ddab/PG	40
2.5.7.2	Effect of nitromethane concentration on eNOSoxy-mediated catalytic reduction	42
2.5.7.3	Comparison of the effect of different nitroalkanes on the catalytic efficiencies of eNOSoxy	43
2.5.8.	Comparison of catalytic efficiencies of iNOSoxy- and eNOSoxy-mediated catalytic reduction for the various nitroalkanes	44
2.5.8.1.	Comparison of the effect of different nitroalkanes on the catalytic efficiencies of iNOSoxy and eNOSoxy	44
2.5.8.2	Comparison of the catalytic efficiency as function of scan rate for eNOSoxy- with iNOSoxy-mediated reduction of nitroalkane	46
2.5.9	Michaelis-Menten Kinetics	49

CHAPTER III
EFFECT OF NITROALKANES ON THE CATALYTIC SYNTHESIS OF
NITRIC OXIDE (NO) BY iNOSoxy

3.1. Introduction.....	56
3.2 The Griess assay.....	59
3.3 Results.....	61
CORRELATION OF NOSoxy-MEDIATED CATALYTIC REDUCTION	
OF NITROALKANES AND OBSERVED of NINHIBITION OF NOS REACTION.....	63
REFERENCES.....	65

LIST OF FIGURES

Figure 1.1 Cysteinato-iron(III)protoporphyrin-IX prosthetic group in P450s	8
Figure 1.2 Inducible Nitric Oxide Synthase monomer (PDB database entry# 1NOS).....	10
Figure 1.3 Endothelial Nitric Oxide synthase (Dimer) (PDB database entry# 1NSE)	11
Figure 2.1 The three-electrode electrochemical cell used the voltammetric characterization of NOSoxy-modified electrodes	24
Figure 2.2 Fabrication of pyrolytic graphite electrode	26
Figure 2.3 Cyclic Voltammogram of iNOSoxy in ddab on PG electrode at pH 5.5 in acetate buffer at a Scan rate of 0.1V/s.....	28
Figure 2.4 Cyclic voltammetry of iNOSoxy in ddab on PG electrode in absence and presence of Nitromethane.....	30
Figure 2.5 Cyclic voltammograms of iNOSoxy in ddab film on PG electrode in the presence of increasing nitromethane concentrations.....	31
Figure 2.6 Comparison of catalytic efficiencies as a function of nitromethane concentrations in acetate buffer at pH 5.5	32
Figure 2.7 Catalytic efficiency in the presence of nitromethane, 0.8mM as a function of scan rate.....	33
Figure 2.8 Cyclic voltammograms of iNOSoxy in ddab film on PG electrode with changing scan rates.....	34
Figure 2.9 Effect of scan rate on the potential of the catalytic peak R3.....	35
Figure 2.10 Catalytic efficiency of iNOSoxy-mediated catalytic reduction of the various nitroalkanes as a function of concentration.....	37
Figure 2.11 Catalytic efficiencies of iNOSoxy-mediated reduction of the various nitroalkanes as a function of scan rate.....	38
Figure 2.12 Cyclic voltammetry of eNOSoxy/ddab/PG at pH 5.5 in acetate buffer at scan rate 0.1V/s.....	40
Figure 2.13 Cyclic voltammetry of eNOSoxy in ddab on PG electrode	

in absence and presence of Nitromethane	41
Figure 2.14 Comparison of catalytic efficiencies as a function of nitromethane concentrations in acetate buffer at pH 5.5	42
Figure 2.15 Catalytic efficiency of eNOSoxy-mediated catalytic reduction of the various nitroalkanes as a function of concentration.....	43
Figure 2.16 Comparison of the catalytic efficiencies of iNOSoxy and eNOSoxy as a function of nitropropane concentrations in acetate buffer at pH 5.5	45
Figure 2.17 Catalytic efficiencies of iNOSoxy and eNOSoxy-mediated reduction at 0.8 mM nitromethane as a function of scan rate in V/s.....	46
Figure 2.18 Catalytic efficiencies of iNOSoxy and eNOSoxy-mediated reduction at 0.8 mM nitroethane as a function of scan rate in V/s.....	47
Figure 2.19 Catalytic efficiencies of iNOSoxy and eNOSoxy-mediated reduction at 0.8 mM nitropropane as a function of scan rate in V/s.....	48
Figure 2.20 Integration of iNOSoxy at the Fe ³⁺ /Fe ²⁺ redox couple; area under the curve is a measure of the charge passed.....	51
Figure 2.21 Integration of the area under the voltammogram at R1 of iNOSoxy/ddab/PG taken at 5mV/s.....	52
Figure 2.22 Catalytic efficiency of iNOSoxy-mediated catalytic reduction of the various nitroalkanes as a function of concentration to obtain the K _m values.....	53
Figure 2.23 Catalytic efficiency of eNOSoxy-mediated catalytic reduction of the various nitroalkanes as a function of concentration to obtain the K _m values.....	56
Figure 3.1 Comparison of iNOSoxy activity (NO synthesis) in the presence of nitromethane (black solid squares), nitroethane (red solid circles), and nitropropane (blue solid triangles)	

at various concentration levels. Data are averages of three trials.

Bars represent standard deviations.....60

Figure 3.2 Comparison of eNOSoxy activity (NO synthesis) in the presence of nitromethane (black solid squares). Data are averages of three trials. Bars represent standard deviations.....61

Figure 3.3 Comparison of the normalized enzyme activity of iNOSoxy (black solid squares) with eNOSoxy (black solid circles) in the presence of Nitromethane. Data are average of three trials. Bars represent standard deviations.....62

LIST OF SCHEMES AND TABLES

Scheme 1.1 Cytochrome P450–redox partner electron-transfer complex	9
Scheme 1.2 General electron transfer pathway during the NOS reaction	12
Scheme 2.1 Conversion of nitroalkanes to corresponding hydroxylamines	16
Table 2.1 The Km Values for iNOSoxy and eNOSoxy in the presence of nitroalkanes	54
Scheme 3.1 Nitric oxide biosynthesis	57
Scheme 3.2 Griess assay reaction	58

ABBREVIATIONS

CaM: Calmodulin

CPR: Cytochrome P450 reductase

CYPs: Cytochrome P 450s

ddab: didodecyldimethylammonium bromide

DTT: Dithiothreitol (Name: (2*S*,3*S*)-1,4-bis(sulfanyl)butane-2,3-diol)

eNOSoxy: Oxygenase domain of endothelial nitric oxide synthase

eNOS: Endothelial nitric oxide synthase

EPSP: (3-[4-(2-Hydroxyethyl)-1-piperazinyl] propanesulfonic acid)

FAD: Flavin adenine dinucleotide

FMN: Flavin mononucleotide

HMG-CoA: 3-hydroxy-3-methylglutaryl-coenzyme A

H₄B: Tetrahydrobiopterin (systematic name: (6*R*)-2-Amino-6-[(1*R*,2*S*)-1,2-dihydroxypropyl]-5,6,7,8-tetrahydropteridin-4(1*H*)-one)

iNOSoxy: Oxygenase domain of inducible nitric oxide synthase

IPTG: isopropyl- β -D-1-thiogalactopyranoside

NAD: Nicotinamide adenine dinucleotide

NADH: Nicotinamide adenine dinucleotide (reduced form)

NADPH: Nicotinamide adenine dinucleotide phosphate (reduced form)

NED: N-1-naphthylethylenediamine dihydrochloride

NO: Nitric Oxide

NOHA: N-Hydroxy-L-Arginine

NOS: Nitric oxide synthase

NOSoxy: Oxygenase domain of nitric oxide synthase

nNOS: Neuronal nitric oxide synthase

PDB: Protein database

PG: pyrolytic graphite

SAMs: Self-assembled monolayers

TNT: Trinitrotoluene

GENERAL INTRODUCTION

Organic Nitroalkanes (Nitromethane, Nitroethane and Nitropropane) are constantly released into the environment as they are used by a variety of industries. For example, they are used by drag racers and hobbyists as fuel in race cars, in the manufacture of explosives like TNT[1], in the pharmaceutical industry, and in the manufacture of pesticides and fungicides [2]. Nitroalkanes are considered to be harmful to the human body. Enough evidence about the health hazards of exposure to nitroalkanes accumulated from workers directly exposed and from the general population[2].

Nitroalkanes released through spills from industries, during their transportation or from the emissions of cars and rockets, can enter the body by inhalation, skin contact or through food, causing serious side effects to the human body[3]. These side effects range from normal problems like nausea and headaches, to serious problems like convulsions and even death when inhaled in a chronic manner. At the cellular level, they can cause problems like mutagenicity[4] and genotoxicity[5] with associated outcomes such as tumorigenicity[6], and carcinogenicity[7].

The mechanism by which these organic nitrocompounds get converted into harmful compounds is still unclear. A large number of drugs and harmful substances are known to be detoxified by cytochrome P450 enzymes (CYP) in the liver where they are metabolized and excreted later on [8]. For example, atorvastatin (Pfizer trade name: Lipitor) which is a 3-hydroxy-3-methylglutaryl-coenzyme A (HMG-CoA) reductase inhibitor, is mainly metabolized by cytochrome P450 3A4[9]. There is also enough evidence that P450 enzymes convert drugs and xenobiotic substances to harmful substances. The study of activation of nitroalkanes by cytochrome P450 and cytochrome P450-like metalloenzymes is of interest in this regard.

Nitroalkanes are perceptibly acidic compounds. The dissociation of a proton from a nitroalkane produces the nitroalkane anion, or nitronate, which have considerably different chemical and physical properties from those of the parent nitroalkane [10].

Previous research has shown how cytochrome P450 enzymes transform nitroalkanes into reactive substances [11]. The present study investigates the catalytic reduction of nitroalkanes by the oxygenase domain of iNOS and eNOS (iNOSoxy and eNOSoxy respectively), which also have a structural similarity to P450 metalloenzymes. Also, we explored if there is any correlation between the extent of NOSoxy-mediated electrocatalytic reductions of nitroalkanes and their effect on the inhibition of the NOS catalytic reaction by iNOSoxy and eNOSoxy.

Traditional methods of enzyme activity study include assays to determine initial rates or transient kinetics using techniques such as spectrophotometry, light scattering, fluorometry, chemiluminescence, calorimetry, chromatography and radiometric analysis[12]. These methods can resolve enzyme mechanisms in the concentration and time domains by measuring the concentration change of the substrate or product versus time.

The catalytic reduction of nitroalkanes mediated by NOSoxy, as well as the NOS enzymatic reaction, both involve electron exchanges. Electrochemical methods can therefore be used to monitor these catalytic reactions. Electrochemical methods have the advantages of being sensitive, and relatively straightforward. To this end, we used the surfactant film methodology[1] [13], to immobilize iNOSoxy and eNOSoxy metalloproteins on the surface of pyrolytic graphite (PG) electrodes. We use this system to study iNOSoxy- and eNOSoxy-mediated catalytic reduction of nitroalkanes[14, 15]. In biological systems, enzymes such as cytochrome P450s (CYPs) use electron donors such as NADPH or NADH to perform their enzymatic activity. Direct electrochemical methods such as the surfactant method circumvent this need by providing reducing equivalents to the metalloenzymes directly from the underlying solid electrode [16, 17]. We could thus study the enzymatic reactions by monitoring electron flow directly from the electrode in the presence of varying amounts of substrate.

We used this method to study the electrocatalytic reduction of nitroalkanes mediated by iNOSoxy and eNOSoxy to derive corresponding K_m and k_{cat} values. We compared and contrasted the catalytic data in light of the inhibitory effect of various

nitroalkanes on the NOS reaction as catalyzed by iNOSoxy and eNOSoxy. The nitroalkanes we considered in this study are the three basic aliphatic nitro compounds: nitromethane, nitroethane, and nitropropane.

PROTOCOL FOR THE EXPRESSION AND PURIFICATION OF INDUCIBLE AND ENDOTHELIAL NITRIC OXIDE SYNTHASE OXYGENASE DOMAIN (iNOSoxy and eNOSoxy)

The recombinant nitric oxide synthase oxygenase domain of (iNOSoxy or eNOSoxy) was purified from *Escherichia coli* using previously published protocols [18]. The *Escherichia coli* culture with the cDNA encoding iNOSoxy or eNOSoxy is grown in Terrific Broth (TB) medium in flasks that were previously autoclaved.

The seed culture was grown at 37°C supplemented with ampicillin. When the cells reached an appropriate density, the expression of the recombinant protein was induced by adding isopropyl- β -D-thiogalactopyranoside (IPTG). After 10-12 hours, the cells were harvested by centrifugation at 40°C and resuspended in the lysis buffer. The cells were repelleted, resuspended, and then sonicated to release the protein expressed. The suspension is centrifuged and the supernatant was collected. Ammonium sulfate (0.3mg/ ml volume of the protein) was used to precipitate the proteins out of the mixture. The suspension is centrifuged to collect the precipitated protein into pellets. Histidine-Tag affinity chromatography was used to separate the iNOSoxy or eNOSoxy from the protein mixture. The protein solution obtained was dialyzed overnight and then concentrated as needed. The concentration of the enzyme was determined using the P450 assay [19]. EPPS (3-[4-(2-Hydroxyethyl)-1-piperazinyl] propanesulfonic acid) buffer was taken as blank and iNOSoxy or eNOSoxy in EPPS buffer was used as sample. Absorption at the *Soret* band at 420 nm is first recorded. The cuvette is then saturated with carbon monoxide and then reduced using sodium dithionite. The resulting Fe^{2+} state of eNOSoxy or iNOSoxy forms the carbonyl complex that is quantified at 444 nm using known extinction coefficient. The typical concentration of the protein in our preparations was about ~120 μM

Determination of the enzymatic activity by using Griess assay:

The activity of the enzyme was determined using the Griess assay[20]. All the reaction ingredients needed for the formation of NO (i.e. H_4B and the substrate N-hydroxy-L-arginine (NOHA) were added first). The reaction was triggered by adding H_2O_2 and then, catalase was added to stop the reaction after a desired period of time (typically 12-15 min). The reaction mixture was stored on ice until it was analyzed. The nitric oxide formed is spontaneously converted to nitrite (NO_2^-) as a stable end product. The Griess reagents, sulfanilamide and N-1-naphthylethylenediamine dihydrochloride (NED), are added to convert the nitrite present to a red-pink colored diazo compound that is quantified using UV-vis[21]. The specific activity for iNOSoxy was around $63.5 \text{ nmol (NO).min}^{-1}.\text{nmol (enzyme)}^{-1}$ and $2.20 \text{ nmol (NO).min}^{-1}.\text{nmol(enzyme)}^{-1}$ for eNOSoxy.

CHAPTER I

NOS OXYGENASE MEDIATED NITROALKANE ELECTROREDUCTION

1.1 Introduction

Nitroalkanes are widely used substances for a variety of industrial applications. They are used as fuel with methanol and paraffins by drag racers and hobbyists, in the manufacture of explosives more powerful than dynamites, in the pharmaceutical industry, and in the manufacture of pesticides, fungicides, vinyl inks, adhesives and electrostatic paints[22]. Primary and secondary nitroalkanes act as excellent building blocks for the synthesis of complex molecules. Hence, they are used for the synthesis of larger complexes in a variety of reactions[23].

While organic nitrocompounds have a variety of applications, their toxicity is not well understood, and many aspects of their interaction with biological systems need close examination. They are considered a serious environmental hazard and are often released into the environment through spills, transportation, and as emissions from cars. When inhaled, these compounds are detrimental to human health. While acute exposures are not a major risk, chronic or prolonged exposure can lead to induced methemoglobinemia[24]. This results in the decreased oxygen carrying capacity of blood and causes headache, nausea, vomiting, and convulsions. Although the type of toxicity is compound-specific, the reported toxicological effects are mutagenicity[4] and genotoxicity[5] with associated outcomes such as tumorigenicity[6], neuropathy[25], and carcinogenicity[1].

To deal with xenobiotic compounds that inevitably find their way into tissues, animals have evolved systems to eliminate these toxic compounds. Enzymatic systems within the human body often remove the xenobiotic harmful substances by converting the lipophilic chemical compounds into hydrophilic products that are readily excreted. [26]. These reactions often detoxify poisonous compounds; however, in some cases, the intermediates of xenobiotic metabolism can themselves be the cause of toxicity.

1.2 Cytochromes P450:

Cytochromes P450 (CYPs) are a gene superfamily of heme proteins found in all *eukaryotes*, most *prokaryotes*, and *archaea*. They are known to metabolize a wide array of organic molecules[8]. CYPs use a variety of small and large molecules as substrates in enzymatic reactions. The term P450 is derived from the spectrophotometric peak at the wavelength of the absorption maximum of the enzyme (450 nm) when it is in the reduced state and complexed with carbon monoxide (CO)[27]. Previous studies have shown that the nitroalkanes can be converted into harmful substances by CYPs[1].

Cytochrome P450s can be classified into many classes [6, 28] including but not limited to microsomal, mitochondrial, and bacterial P450 systems,

Most CYPs can metabolize multiple substrates and are involved in multiple reactions. this enables them to catalyze the transformation and degradation of a large variety of molecules[28]. The cytochromes P450s constitute a large family of cysteinato-heme enzymes, and play a key role in the oxidative transformation of endogenous and exogenous molecules[23]. In all these cysteinato-heme enzymes, the prosthetic group is an iron (III) protoporphyrin-IX coordinated to the protein by the sulfur atom of a proximal cysteine ligand (Figure 1.1). P450 reactions of biological significance include steroid biogenesis, drug metabolism, procarcinogen activation, xenobiotic detoxification and fatty acid metabolism[29].

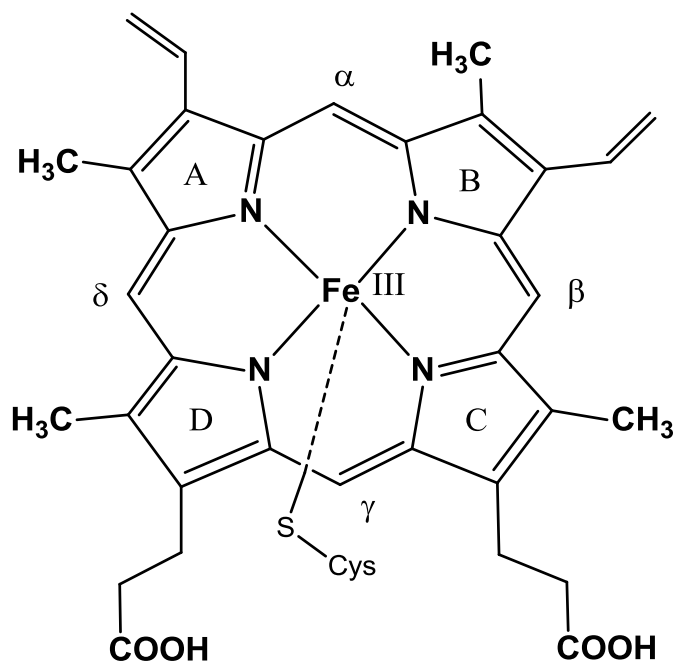
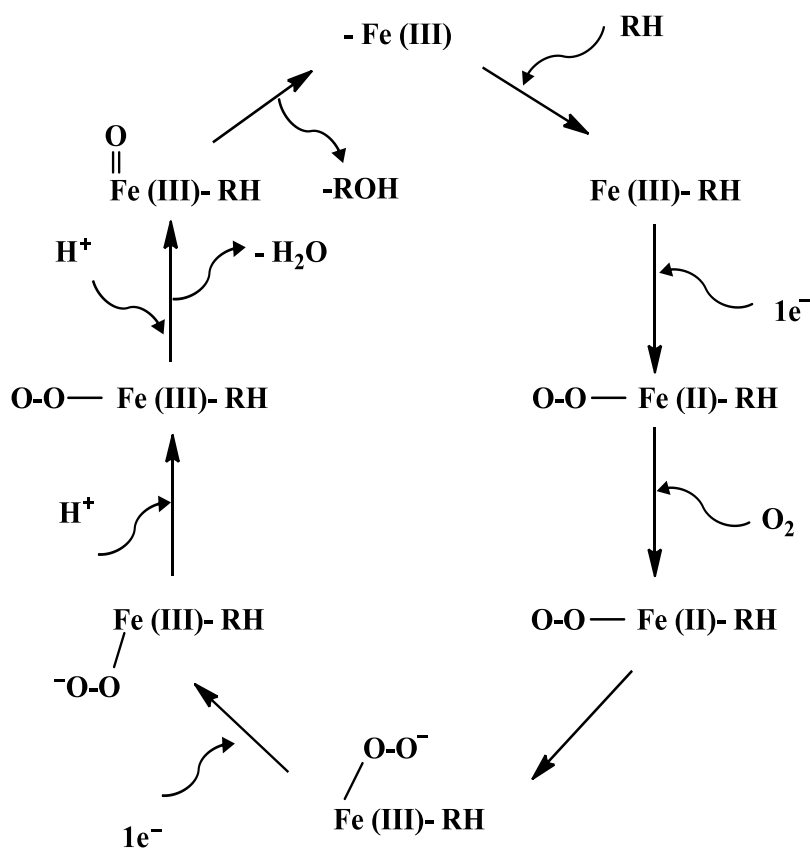


Figure 1.1 Cysteinato-iron(III)protoporphyrin-IX prosthetic group in P450s

Under aerobic conditions, P450 enzymes activate molecular oxygen, insert one of the oxygen atoms into a substrate (RH in Scheme 1.1), and reduces the second oxygen to a water molecule, utilizing two electrons that are provided by NAD(P)H via a reductase protein[30]. Since only one of the two oxygen atoms initially present in O_2 remains in the oxidized substrate, P450s are called monooxygenases. Molecular oxygen itself is unreactive toward organic molecules at low temperatures due to high kinetic barrier. Consequently, living systems mainly use enzymes that can activate dioxygen and performs the desired oxidation reactions. This modification can be achieved by metal-dependent oxygenases, like cytochromes P450 and other non-heme metalloenzymes (e.g., methane monooxygenase), or by flavin-containing enzymes that do not possess a metal-based prosthetic group[31].



Scheme 1.1 Cytochrome P450–redox partner electron-transfer complex

However, not all xenobiotic compounds take the oxidative metabolic pathway. Some nitro-compounds can be reductively activated by cytochrome P450s. Nitrocompounds can either be reduced or oxidized depending on the enzyme involved. They can be reduced by cytochrome P450s through catalytic electron transfer[32].

1.3 Nitric Oxide Synthase:

Nitric oxide synthases have been the subject of intensive studies[33]. The mode of action, distribution in different tissues, organs and species as well as comparisons between the function of the three known isoforms at the molecular level has been the main focus. More than 30,000 papers have been published in the past 10 years related to Nitric Oxide Synthases (NOSs). NOSs are the enzymes responsible for the synthesis of nitric oxide (NO) from L-arginine in mammalian tissues. These enzymes are remarkable for the complexity of the catalytic reactions they carry out and the range of physiological roles in which they are involved[34]. NOSs play a crucial role in the control of blood flow, memory, and the immune response.

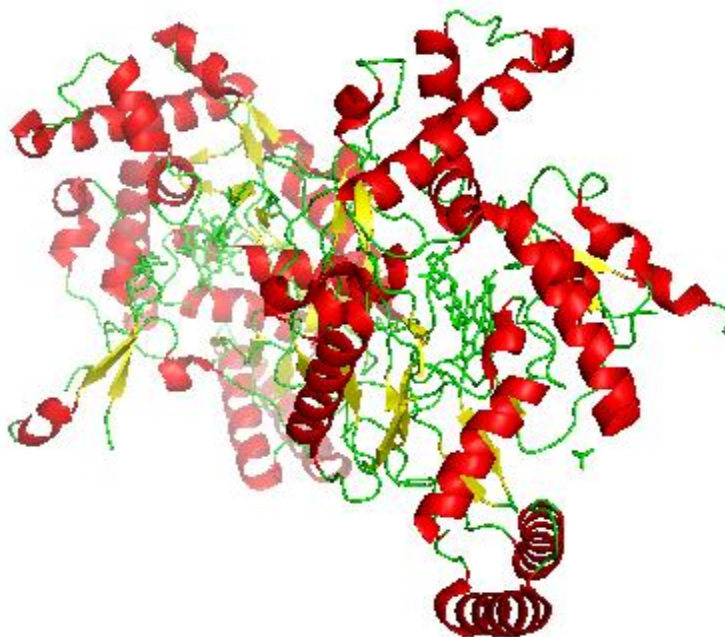


Figure 1.2 Inducible Nitric Oxide Synthase dimer (PDB database entry# 3E7T).

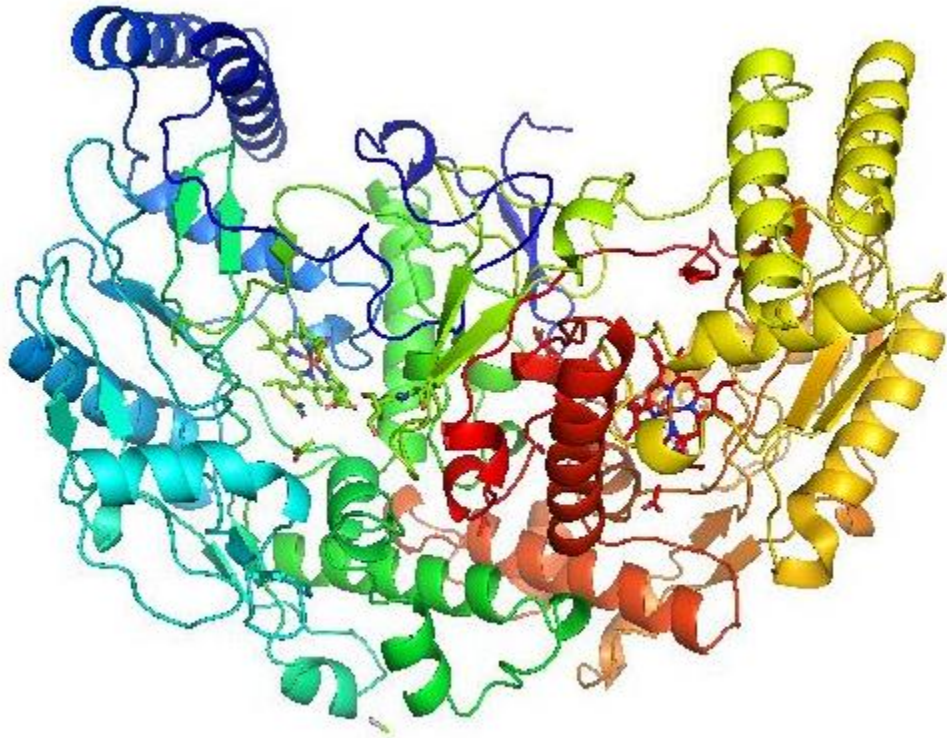
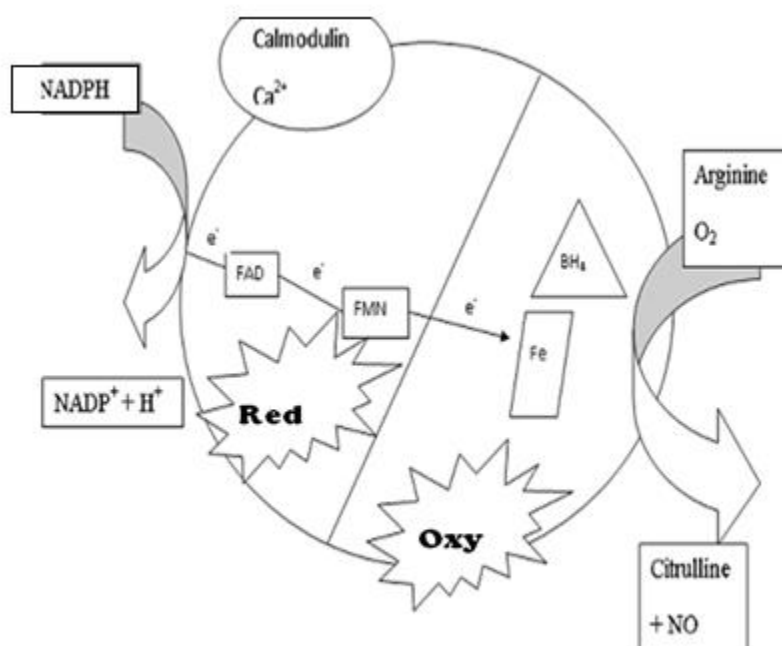


Figure 1.3 Endothelial Nitric Oxide synthase (Dimer) (PDB database entry# 1NSE).

NOSs are modular enzymes that consist of an N-terminal oxygenase domain (Figures 1.2 and 1.3) and a C-terminal reductase domain. Catalysis takes place at a cysteinyl sulfur-coordinated heme in the oxygenase domain. The heme iron binds O_2 as a sixth ligand in the distal pocket, which also serves as the site for substrate binding. In close proximity, tetrahydrobiopterin (symbolized as H_4B) is bound as an additional cofactor. The required electrons are provided by the reductase domain, which shuttles

electrons from NADPH to the heme via two flavin cofactors, one FAD moiety that accepts electrons two at a time from NADPH, and one FMN moiety that transfers them one at a time to the heme catalytic center [35] (Scheme 1.2). The two domains are separated by a short amino acid sequence that binds calmodulin (CaM) to enable interdomain electron transfer. NOS is only active as a homodimer, because electron transfer can only occur from the reductase domain of one subunit to the oxygenase domain of the second subunit.



Scheme 1.2 General electron transfer pathway during the NOS reaction [31]

There are three distinct isoforms of NOS, which differ both in their structure and function. Endothelial NOS (eNOS), neuronal NOS (nNOS) and inducible NOS (iNOS)

[36]. The three NOS isoforms are characterized by regions of high homology, but at the same time each isoform exhibits distinctive features that reflect its specific function. The Ca^{2+} -activated calmodulin in all nitric oxide synthases plays an essential role in dimerization. In its absence, NOS exists as monomers. Dimerization is also supported by the substrate arginine and by the tetrahydrobiopterin cofactor. The X-ray crystal structures of NOS oxygenase domains confirmed that the heme is bound to a proximal cysteine thiolate ligand, akin to the family of P450 enzymes (Figures 1.2 and 1.3). Evidence obtained from studying the fluorescence dynamics of flavins suggests that the heme is also essential in the interaction between the reductase and oxygenase domains, which form an interface in the quaternary structure[37].

1.4. Similarities between nitric oxide synthases and P450 enzymes:

The Nitric oxide synthases shows some similarities and at the same time, exhibit striking differences with P450 enzymes. Strictly speaking, the label cytochrome P450 stands for a widely distributed group of closely related functional enzymes that also have common structural features, including the heme-cysteine thiolate ligation. Only in this limited structural sense NOSs are similar to the P450 family. Also, a superficial resemblance may stem from the fact that NOSs catalyze mono-oxygenation steps of its substrate. The most striking among the similarities between P450 and NOS is the fact that both the NOS oxygenase domain (NOSoxy) and mammalian (microsomal) P450 utilize the same electron donor as a redox partner. Whereas the oxygenase domains of iNOSoxy and P450 are relatively unrelated, the reductase domain (NOSred) and cytochrome P450 reductase (CPR) share 60% sequence homology[38]. In contrast to most P450s, active NOS enzymes are dimeric. Despite the sequence homologies, there are a number of notable differences between NOSred and CPR. Specifically, NOS is equipped with a number of insertions and extensions that are specific for NOS, and that vary between the isoforms.

Structural elements of nitric oxide synthases like the calmodulin binding sequence at the N-terminal of the reductase domain, the C-terminal NADPH binding site, the FMN domain and the small insertions between FAD and FMN domains form the core of the reductase domain of nitric oxide synthases and show similarities with cytochrome P450 reductase enzymes.

Spectroscopically, the similarities between NOS oxygenases (NOSoxy) and P450s, or rather between their respective heme prosthetic groups, outnumber the differences. Whereas most oxyferrous complexes of thiolate-ligated hemoproteins including P450 have Soret maxima at about 418 nm [39], the corresponding peak for NOS is usually at 428 nm, although a more P450-like position at 418nm is observed under some conditions. This difference in the position of the Soret band of the oxyferrous complex could be a prominent distinction. It is not yet clear what is causing the remarkable red shift and why it is sometimes absent. Based on these similarities and differences, it is worthwhile to explore to what extent nitric oxide synthases can act like P450s in activating nitroalkanes. In a related aspect, we would like to know to what extent nitroalkanes interfere with and inhibit the molecular function of NOSs and nitric oxide synthesis.

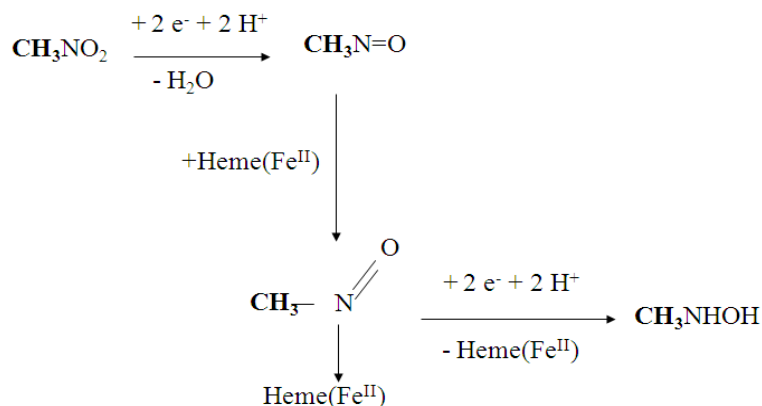
CHAPTER II

iNOSoxy AND eNOSoxy MEDIATED NITROALKANE ELECTROREDUCTION

2.1. Introduction

Nitroalkanes are considered a serious hazard both to the environment and to human health. While acute exposures are not a major risk, chronic or prolonged exposure can lead to adverse reactions and an onset of pathological conditions, including decreased oxygen carrying capacity of blood with symptoms such as headache, nausea, vomiting, and convulsions [40].

Nitroalkanes are electroactive and can be converted to the corresponding hydroxylamines and amines by a series of proton-coupled electron transfers. This reduction can be catalyzed by heme or heme-proteins as shown in scheme 2.1.



Scheme 2.1 Conversion of nitroalkanes to corresponding hydroxylamines [41]

Previous studies show that the P450 enzymes can convert nitroalkanes into hydroxylamines[42]. The electrons required for the reaction are provided by the flavoprotein reductases.

Nitric oxide synthases (NOSs) exist as homodimers. Each monomer consists of two major regions: an N-terminal oxygenase domain with a heme-thiolate catalytic center, and a multi-domain C-terminal reductase domain, which is homologous to P450 reductases and other flavoproteins. The reductase domain contains FMN and FAD binding subdomains and a binding site for NADPH, which is the source of reducing equivalents. The interdomain linker between the oxygenase and reductase domains contains a calmodulin-binding sequence. The oxygenase domain is a unique extended beta sheet cage with binding sites for heme and a pterin cofactor. Binding of calmodulin appears to act as a "molecular switch" to enable electron flow from flavin prosthetic groups in the reductase domain to the heme. Given the structural similarity at the heme domain between the P450 proteins and NOSs, the catalytic reduction of nitroalkanes can be conceptually mediated by NOSs using electrons from its flavoprotein reductase.

2.2. Electrochemical methods and application to the study of redox proteins

P450s use electron transfers to perform the reductive activation of substrates. Electrochemical methods can be used to monitor the transfer of reducing equivalents that drive the catalytic reaction. Usually, redox partners are needed in electron-driven catalytic transformations. However, the electrode surface can play the role of electron source, which also provides a means to monitor the corresponding catalytic reductions. Efficient coupling of the large biological enzyme to the electrode surface is critical for this type of electron transfer to happen. In fact, direct electron transfer to large biomolecules such as proteins and enzymes at an ordinary electrode surface is usually very slow. However, this barrier may be overcome by using redox promoters such as conjugated and aromatic organic molecules [13], by directly tethering the redox proteins to electrode surfaces, or by embedding them in thin films on electrodes.

Electrochemical methods comprise a collection of useful measurement tools. A central feature of these methods involves an electrode that provides an interface where some form of charge-transfer process occurs. This charge-transfer process is characterized by potential and/or current signals that can be measured and used to monitor coupled chemical processes in the immediate vicinity of the electrode surface.

Broadly speaking, electrochemical methods can be divided into two groups: measurements that do not involve current, known generally as potentiometric methods, and measurements that involve current flow at an electrode under potential control.

During an electrochemical measurement, the oxidation and reduction of the solution components at the surface of the electrode, gives an electric signal which is used to derive information redox entities in the immediate vicinity of the electrode. When a molecule undergoes oxidation at the electrode surface, electrons flow from the molecule into the electrode material, is measured in the form of electrical current that reports on the magnitude of the electron exchange. While in an electrochemical reduction, electrons flow from the electrode to the analyte of interest. Therefore, the electrode can be viewed as either an oxidizing agent or a reducing agent, depending on

the direction of current flow, which is a result of the imposed potential and the nature of the analyte near the electrode.

Cyclic voltammetry (CV) is widely used in electroanalytical studies and mechanistic investigations. As the name implies, the potential is swept from an initial potential to a final potential and then returned to the initial or to a different potential, usually at the same scan rate. The current measured continuously during the scan is reported against the applied potential. Hence, the technique provides voltammetric information (current vs. potential) about the substance in contact with the electrode and the various chemical processes that are triggered by electron transfers to or from the electrode. This is useful for both qualitative and quantitative identification and also for the detailed mechanistic study of electron-driven chemical and catalytic transformations.

CYP enzymes use NADPH or NADH as electron donors to perform their enzymatic activity. As stated above, if enzymes such as CYP can be connected to solid electrode surfaces by a bridge or other promoters, electrons can be exchanged with the underlying electrode, thus shortcutting the need for soluble electron donors or mediators in the system. We can thus study enzymatic reactions by providing the electrons directly from the electrode. The current response on the electrode is directly related to the rate of the reaction and the amount of substrate being processed. In this dynamic technique, thermodynamic information on the active site of the enzyme is obtained from electrode potential, and information on enzymatic kinetics is obtained from the current. When direct electron transfer to large redox proteins and enzymes on an electrode is possible, the amount of sample needed can be very small; this is a direct result of the high sensitivity of electrochemical techniques.

Direct electrochemistry can be a very useful tool for the study of the properties of proteins and the nature of reactions in which they participate. As hinted above, direct electron transfer to large redox proteins is often slow due to many reasons. One reason is the fact that the electroactive group is often buried within the protein shell. Denaturation of proteins and adsorption of protein debris on the electrode surface is another reason that slows down the direct electron transfer. The unfavorable orientation of the protein

and the electroactive group embedded within it may be a third reason for the sluggish direct electron exchange. Here the heme group in the nitric oxide synthase is relatively buried within the protein, which prevents its direct interaction with the electrode surface for electron transfer [43]

A general approach to enhance the rate of direct electron transfer to large biomolecules such as proteins is to couple them to the electrode surface with molecular wires (i.e. conjugated molecules) or affix them in thin films or layers that facilitate electron exchange. Methods such as self-assembled monolayers, biocompatible polymer films, surfactant bilayers, redox nanoparticles, and polyelectrolyte layer-by-layer films have been applied to immobilize redox proteins at the electrode surface [44]. One method that proved to be versatile and straightforward is the surfactant film methodology[45]. Due to low concentration of protein samples used, methods that allow the formation of multiple layers and increase the effective electroactive proteins near the electrode surface are of interest. Such configuration is offered by the multiple layers of surfactant film which trap a relatively large amount of the redox protein under consideration[43]. In the past, we have used surfactants such as didodecyldimethylammonium bromide (ddab) or phosphatidylcholine derivatives, which provide thin stable films as a microenvironment for enhanced electron transfer with the redox protein[45]. Particularly, ddab film forms ordered bilayer structures, and provides a configuration which can increase the protein concentration at the electrode interface and also facilitates appropriate orientation for electron exchange[17]. At the same time, the ddab films allow for the needed exchange of electrolytes with the solution during electrochemical reactions.

2.3 Protein immobilization method

Before the development of biomolecule immobilization methodologies, electrochemical studies of redox proteins and enzymes were carried out in solution and the signal obtained directly at the working electrode was very slow. In other cases

electron exchange was facilitated by small redox mediators[46]. This approach requires large amounts of precious protein samples and, with the quality of current signal obtained from the slow electron transfer it is impossible to gain useful kinetic or thermodynamic insights. The protein immobilization method confines the protein on the surface of working electrodes instead of having a protein in solution. This approach not only saves a lot of protein sample, but also enhances the electrochemical signal. The early feasibility of direct (non-mediated) electron transfer to and from redox proteins spurred electrochemical investigations of metalloproteins and other redox proteins in many directions, and opened valuable doors for the thermodynamic and kinetic studies on electron-driven enzymatic reactions. In addition to enhanced electrochemical signals, the advantages of enzyme immobilization on electrodes include reduced cost and ease of studying the effect of experimental parameters such as pH, as well as the effect of solution-based cofactors and reactants by just dipping the modified electrode in various solutions.

Enzymes and other redox proteins can be attached to an electrode by interactions ranging from reversible physical adsorption and ionic linkages, to entrapment in thin films and lipid bilayers, to more sturdy covalent bonds. Techniques using surface-confined metalloproteins, especially enzymes, at electrode interfaces may not only provide means to construct substrate-specific biosensors and bioreactors, but can also be used to study enzymatic activity of metalloenzymes. The covalent attachments commonly used include amide, ether, thio-ether, or carbamate functionalities.

2.3.1 Formation of covalent bonds

Immobilization of redox proteins through the formation of covalent bonds is well established. An advantage of these methods is that specific reactive residues can be introduced and targeted to allow appropriate orientation of the biological entity on the electrode surface. The targeting approach also helps to avoid alteration of essential catalytic domains or residues.

The array of reactive groups allowing covalent tethering of enzymes and redox proteins to electrodes and matrices is large and dictated by the nature of the redox protein and electrode interface. Chemical coupling of enzymes and redox proteins to polymeric matrices with reactive functional groups is another mode of covalent attachment. The polymeric matrices can covalently attach to the protein of interest on one hand, and react with complementary functionalities on the electrode on the other. Self-assembled monolayers (SAMs) is another method in which alkane thiols spontaneously form on electrode materials such as Au, Pt, and Ag forming stable sulfur-metal bonds [47]. Introduction of appropriate functional groups at the end of these molecular wires provide another method that is used to covalently attach protein molecules. With this configuration and with the right choice of reactive functional groups, one can electronically couple redox proteins of interest with the electrode surface[48].

2.3.2 Adsorption

Another method for the immobilization of proteins is protein adsorption. Proteins adsorb ubiquitously on solid electrode surfaces either as such or with the aid of an appropriate primary adsorbate. The adsorbate forms a layer between the protein and the electrode. The control of the conditions during adsorption is of importance and dictates the extent of coupling and electron exchange with the protein at the surface.

2.3.3 Entrapment in thin films

Entrapment of a redox protein or enzyme within a polymeric network or a thin lipid film allows limited diffusion within the film and intimate communication with the underlying electrode surface. This method differs from the coupling methods, in that the enzyme is not specifically bound to the electrode, matrix, or membrane. However, because of preferred orientations in the film and limited diffusion, the redox protein is able to efficiently exchange electrons with the electrode surface.

2.3.4: Lipid bilayered thin films

Although artificial and may not reflect the native environment for particular enzymes, proteins in lipid films is no innovation but an inspiration from biomembranes in living organisms, which usually are arranged into bilayers with embedded functional proteins. Surfactant molecules is an example and can form ordered bilayers with properties similar to biomembranes. The direct electrochemistry of redox proteins in these biomembrane-like films provides a good model for the study of redox processes in biological systems. Amphiphilic compounds such as didodecyldimethylammonium bromide (ddab) form a water-insoluble bilayered film structure that resembles biomembranes on solid electrode surfaces. Both hydrophilic and hydrophobic proteins or other molecules can be embedded into these thin films[49]. Surfactant ddab and other similar surfactants have proven to form excellent lipid microenvironments for the immobilization of many redox proteins for enhanced electron transfer. Some early examples include myoglobin[1], hemoglobin[50], catalase[51], cytochrome P450cam, cytochrome P450 CYP119, cytochrome P450st30, cytochrome P450BM3, to cite a few. The electrochemical response of these proteins is significantly enhanced compared with bare electrodes. The increased electrochemical response has been ascribed to the fact that the proteins are able to diffuse rapidly through the surfactant film. The ddab surfactant prevents the macromolecular denaturation and the adsorption of the denatured protein on the electrode surface, which can block electron transfer.

NOS oxygenases in surfactant films: The heme in NOS oxygenases (iNOSoxy, eNOSoxy, etc.) undergoes redox changes. Our lab has previously shown that immobilization of NOSoxy proteins in thin surfactant and other types of films on solid electrodes provides a microenvironment for electron exchanges between NOSoxy and the underlying electrode[45]. Our early studies have shown that this system allows for the study of both the kinetic and thermodynamic aspects of redox changes of NOSoxy proteins. As we stated earlier, the lipid bilayer structure provides a biomembrane-like environment in which the protein molecule is trapped while preserving its native structure. We use this configuration to characterize the redox

activity of the heme group in NOS oxygenases and analyze the responses in the absence and presence of nitroalkanes as substrates for catalytic reductions mediated by NOS oxygenases.

2.4. Method

All electrochemical experiments are conducted in a three-electrode system on a BAS 100B electrochemical workstation or a CH Instrument. Ag/AgCl (1M KCl) is used as reference electrode and all potentials are reported versus this reference. A platinum wire is employed as the auxiliary electrode and protein-modified pyrolytic graphite (PG) electrodes are used as working electrodes. Unless specified, all experiments are performed in 0.1M acetate buffer (pH 5.5) containing 0.1M sodium bromide. The solution in the cell is purged with purified nitrogen for at least 15 min prior to electrochemical measurements to remove oxygen from the solution. A nitrogen blanket is maintained to prevent the reentry of oxygen from air[52]. Stirring is maintained between scans [53].

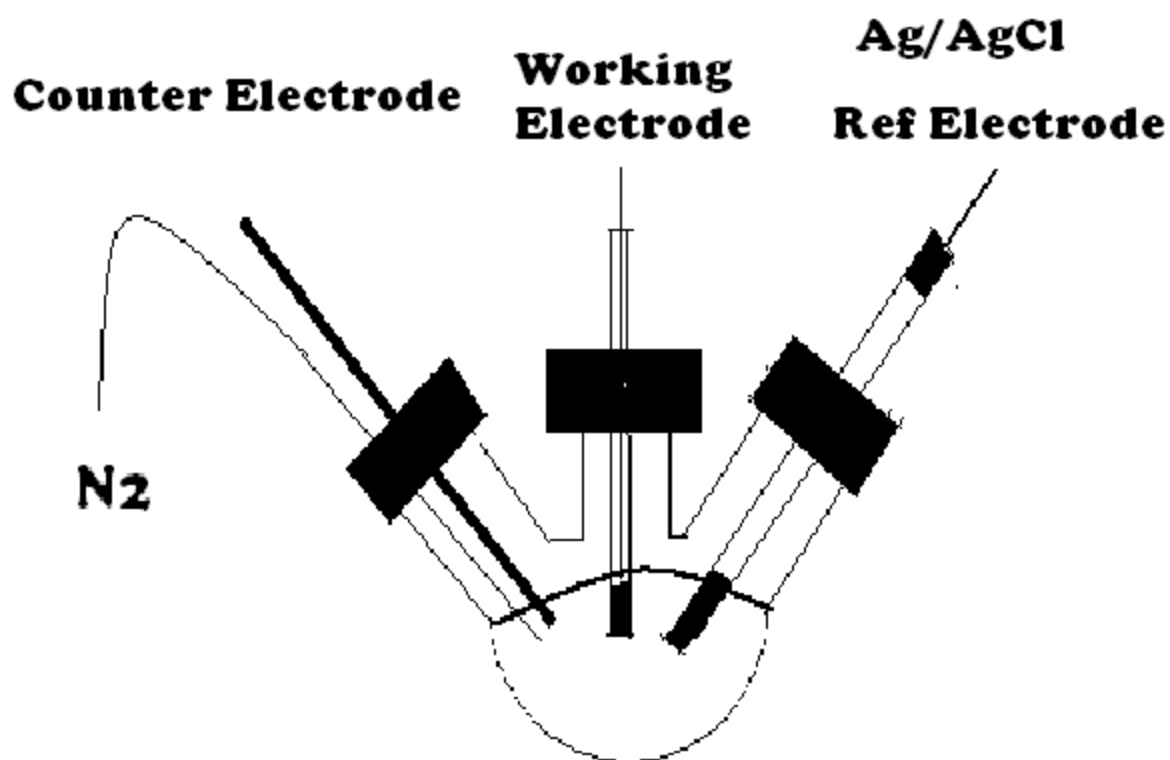


Figure 2.1 The three-electrode electrochemical cell used the voltammetric characterization of NOSoxy-modified electrodes

2.4.1 Materials

iNOSoxy was expressed and purified as described in the protocol for protein purification. Didodecyldimethylammonium bromide (ddab) and all nitroalkanes are from Acros Organics. Nitrogen gas is purchased from PRAXAIR. Deionized water with a resistivity greater than 18 M Ω -cm is obtained from a Barnstead Nanopure system and pyrolytic graphite (Advanced Ceramics) is the material used to make working electrodes as described below.

2.4.2 Fabrication and modification of working electrodes

Pyrolytic graphite (PG) electrodes are constructed as follows. A cylinder of PG was cut perpendicularly to the basal plane from large block using a diamond core drill bit with a diameter of 3 mm as shown in Figure 2.2. A small incision was made on one side of the cylinder for electrical connection with a copper wire which was connected using equal volumes of conductive epoxy and allowed to dry for 24 hours. The graphite cylinder was then inserted into a glass tubing and set in place with non-conductive epoxy and allowed to dry. The non-conductive epoxy was also used to seal the gaps between graphite and glass. The finished electrode was then polished and cleaned as follows: the PG electrode is first polished using 400-grit sandpaper until a fresh basal surface was exposed. The surface of the electrode was then polished successively with 1 μ m, 0.3 μ m and 0.05 μ m alumina slurries. Finally, the electrode is rinsed and briefly sonicated in distilled water to remove any attached alumina particles.

An emulsion of the surfactant is prepared by dissolving enough ddab powder in deionized water to make 10 mM final concentration. The emulsion was then sonicated for at least 2 hours or until the solution becomes clear. A mixture of 10 μ l of 10 mM ddab and 10 μ l of iNOSoxy or eNOSoxy was cast on the electrode surface and the electrode was stored with a cover for 12 hours and then open for another 12 hours at 4°C.

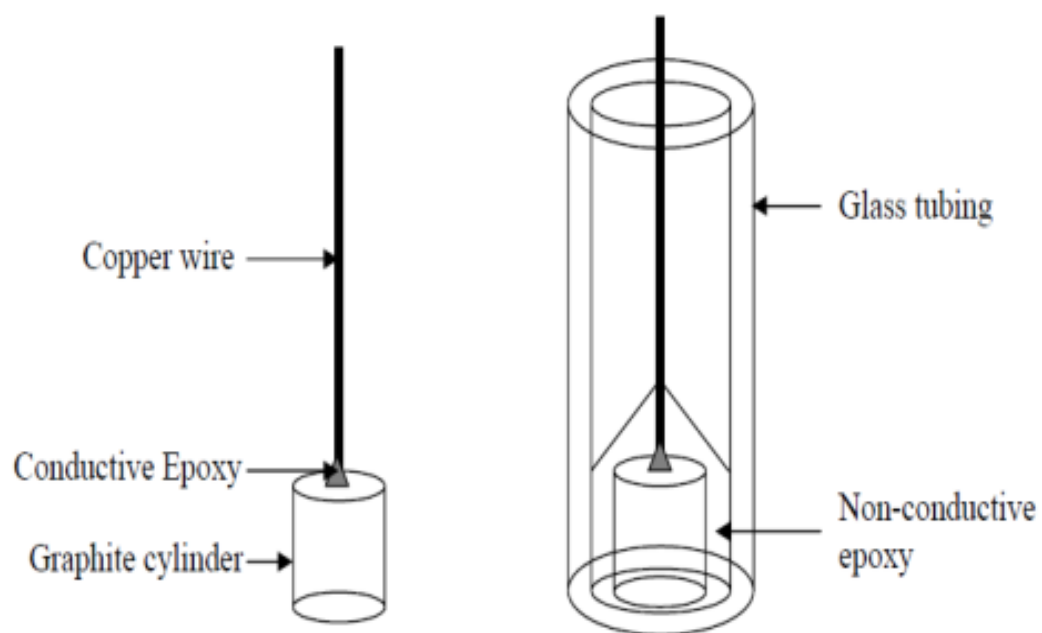


Figure 2.2 Fabrication of pyrolytic graphite electrode

2.5 Results and Discussion

2.5.1 Direct electron transfer to iNOSoxy in surfactant films on pyrolytic graphite and catalytic reduction of nitromethane

Rusling's surfactant films such as ddab films have been employed in the immobilization of many heme proteins, notably myoglobin, hemoglobin and catalase. By immobilizing the proteins on the electrode surface, the electron transfer is significantly enhanced. We used this thin film methodology for the study of redox properties of NOSoxy proteins and to monitor their catalytic reduction of nitroalkanes[45].

Figure 2.3 shows the typical cyclic voltammogram of iNOSoxy in ddab surfactant film in 0.1M acetate buffer at pH 5.5. The voltammogram shows two redox couples. The first redox couple (R_1/O_1) is assigned to the reversible reduction of Fe^{III} to Fe^{II} of the heme center, and occurs at a potential -0.180 V vs. Ag/AgCl (Equation 1). The next couple (R_2/O_2) is assigned to the reduction of Fe^{II} to a formal Fe^I state and occurs around -1.052 V vs. Ag/AgCl (Equation 2). Control experiments with the ddab-only modified pyrolytic graphite electrodes show no redox peaks in the same voltage window.

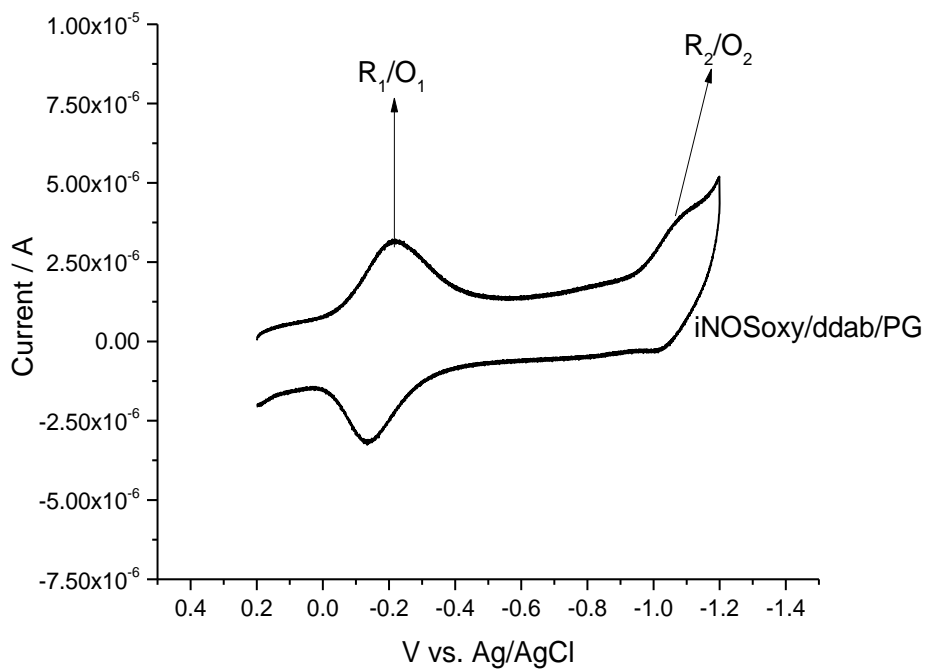


Figure 2.3 Cyclic voltammogram of iNOSoxy in ddab on PG electrode at pH 5.5 in acetate buffer at a Scan rate of 0.1 V/s.

2.5.2 Electrocatalytic reduction of nitromethane catalyzed by iNOSoxy

The cyclic voltammogram of iNOSoxy as described above dramatically changes after adding nitromethane. Upon addition of nitromethane, an irreversible peak, R_3 , appears at -1.0V vs. Ag/AgCl in parallel with the disappearance of the Fe^{II}/Fe^I redox couple[54]. Control experiments on ddab/PG electrodes without iNOSoxy under the same conditions do not show the peak R_3 , which rule out direct reduction of nitromethane at the electrode surface. The R_3 peak current is significantly higher and with a peak potential that is more positive than the R_2/O_2 redox peak. The normalized peak current of R_3 peak (peak current of R_3 divided by the current of R_1) decreases as the scan rate increases. All of these characteristics confirm that the new R_3 peak is a result of the catalytic reduction of nitromethane mediated by iNOSoxy. A similar finding was reported earlier for myoglobin[1]. The peak shape of the catalytic wave, R_3 , is a result of substrate depletion in the film during turnover and subsequent replenishment by diffusion from the bulk.

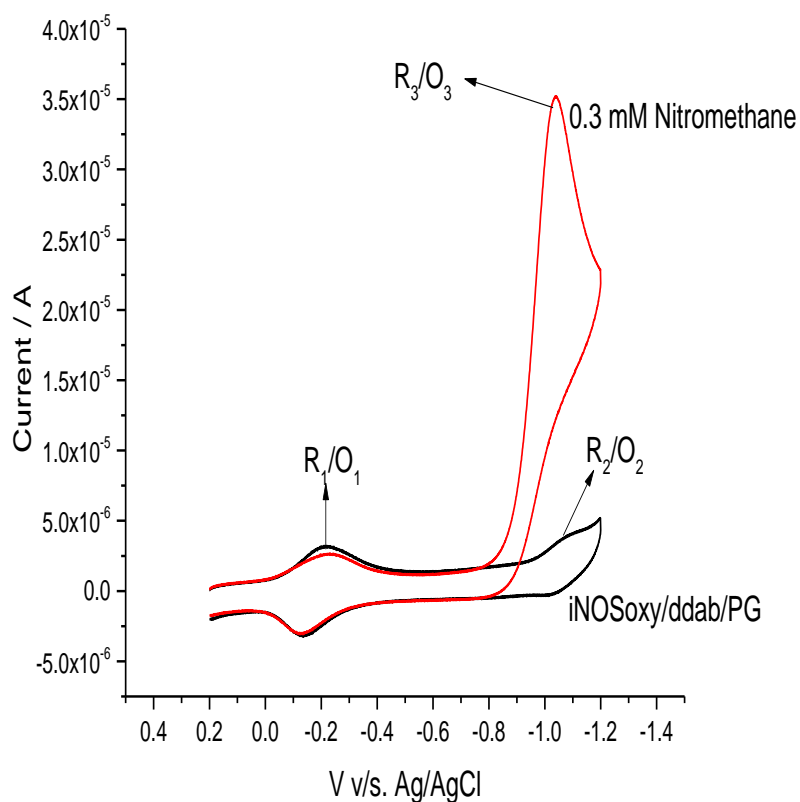


Figure 2.4 Cyclic voltammetry of iNOSoxy in ddab on PG electrode in absence and presence of nitromethane.

2.5.3 Effect of nitromethane concentration:

We compared the iNOSoxy-mediated electroreduction of nitromethane at increasing concentrations ranging from 0.2 mM to 2.0 mM. The catalytic current at the peak R_3 increases with increasing concentration of nitromethane as expected for an electrocatalytic process (Figure 2.5).

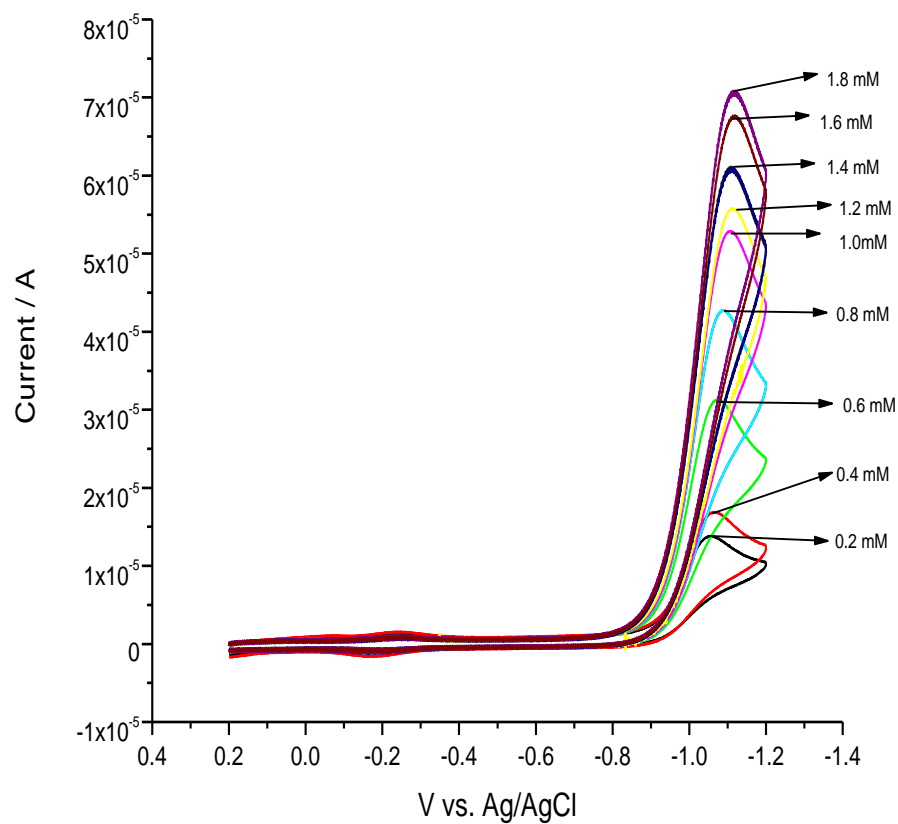


Figure 2.5 Cyclic voltammograms of iNOSoxy in ddab film on PG electrode in the presence of increasing nitromethane concentrations

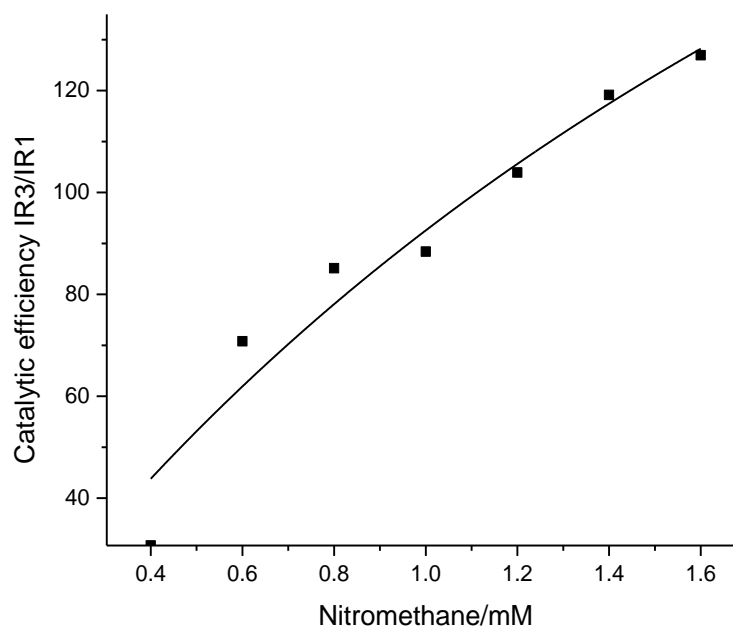


Figure 2.6 Comparison of catalytic efficiencies as a function of nitromethane concentrations in acetate buffer at pH 5.5

One way to monitor the catalytic turnover in this system is to measure the catalytic current and compare it to the current of a monoelectronic peak such as the reversible peak of $\text{Fe}^{3+}/\text{Fe}^{2+}$ redox couple (R_1). The ratio of the catalytic peak current (R_3) to the reversible current of (R_1) defines the catalytic efficiency, which can be used to compare the rate of iNOSoxy-mediated reduction of nitromethane at different concentrations. The catalytic efficiency (I_{R3}/I_{R1}) initially increases and then to curves down with a shape typical of enzyme saturation kinetics (Figure 2.6). Such behavior can therefore be described using the Michaelis Menten model (*vide infra*: nonlinear fitting section).

2.5.4. Effect of scan rate:

We analyzed the effect of scan rate on the iNOSoxy-mediated catalytic reduction of nitromethane. In cyclic voltammetry, increasing the scan rate shortens the timescale within which the catalytic reaction is monitored; as a result the number of catalytic turnovers decreases. As expected, the catalytic efficiency, defined by the ratio (I_{R3}/I_{R1}) is larger at smaller scan rates and gradually drops as the scan rate increases[30]. As shown in Figure 2.7, the increase of scan rate results in a decrease in the catalytic efficiency R_3/R_1 .

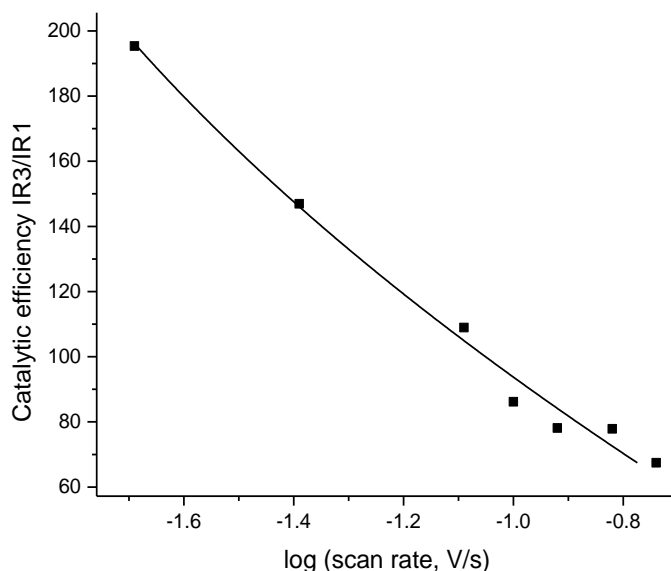


Figure 2.7 Catalytic efficiency in the presence of 0.8 mM nitromethane as a function of scan rate

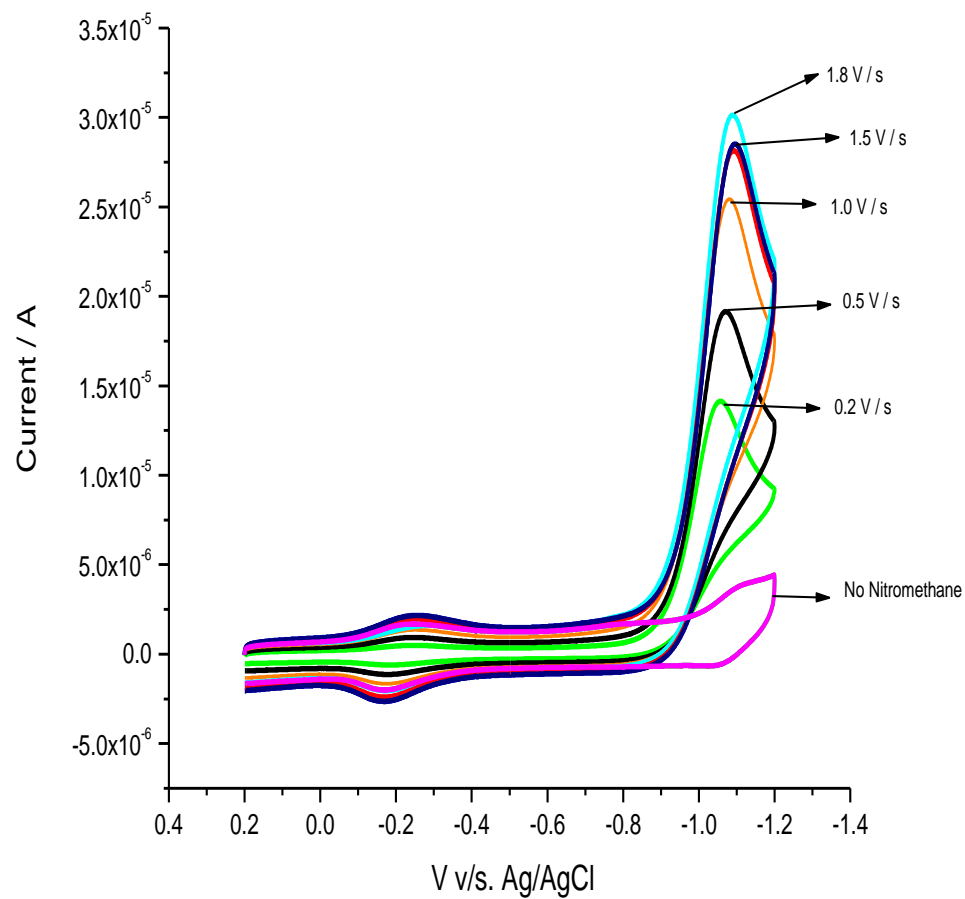


Figure 2.8 Cyclic voltammograms of iNOSoxy in ddab film on PG electrode at various scan rates.

2.5.5 Peak Potentials:

The peak potentials at R_1 and O_1 redox couple were observed at different concentrations of nitromethane. There was no significant change in the peak potential at the R_1/O_1 with varying concentrations of nitroalkanes indicating that there was no significant interaction of the nitroalkanes with the Fe^{3+}/Fe^{2+} redox couple[1].

We plotted the peak potential of the catalytic wave as a function of scan rate. Figure 2.9 shows that the catalytic peak shifts negatively with increasing scan rate. Also, the figure shows that there is an overall negative shift of peak potentials as the concentration of nitromethane is increased. Since we have shown that the iNOSoxy- Fe^{II} -heme potential is not affected by the presence of nitromethane, the negative shift of potentials cannot be rationalized in terms of substrate binding to the Fe^{II} -heme catalytic center.

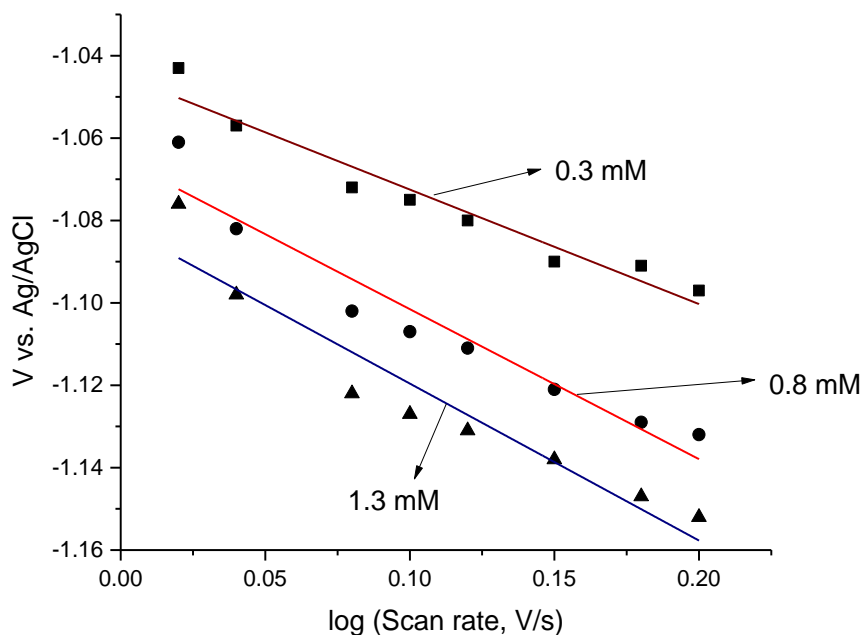


Figure 2.9 Effect of scan rate on the potential of the catalytic peak R_3

2.5.6 Comparison of the electroreduction of different nitroalkanes by iNOSoxy in ddab surfactant films

2.5.6.1 Effect of the nitroalkane concentration:

By comparing the catalytic reduction of three nitroalkanes: nitromethane, nitroethane and nitropropane, we show that all nitroalkanes share a common catalytic feature: As the concentrations of the nitroalkanes increase, there is an increase in the catalytic wave R_3 . However, the rate and extent of increase differs from one nitroalkane to another. Catalytic efficiency was the criterion used to compare the rate of iNOSoxy-mediated reduction of the various nitroalkanes. For all nitroalkanes, the catalytic efficiency initially increases and then curves down with a shape typical of enzyme saturation kinetics. Such behavior can therefore be described using the Michaelis-Menten model (*vide infra*: nonlinear fitting section).

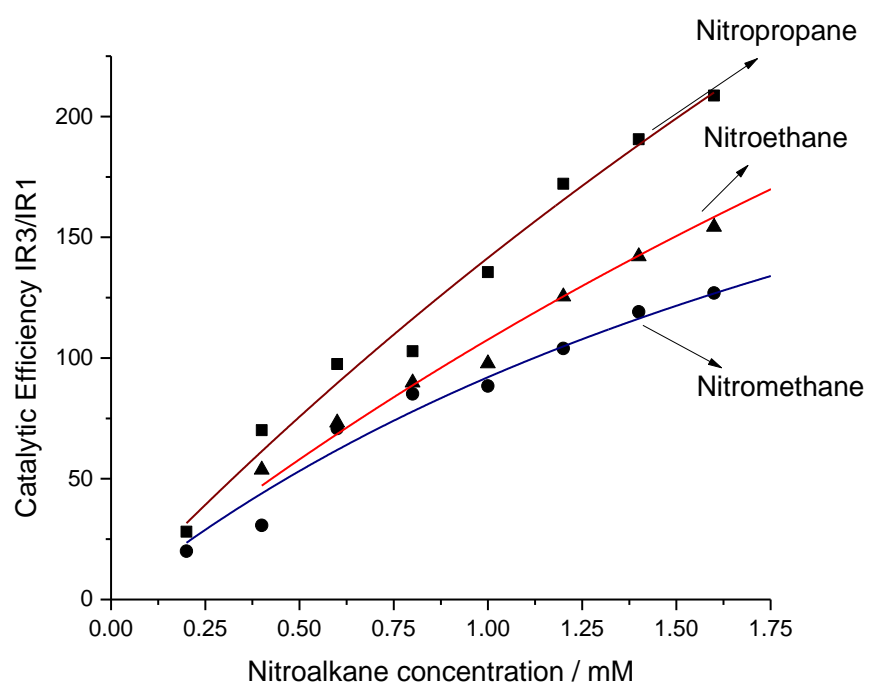


Figure 2.10 Catalytic efficiency of iNOSoxy-mediated catalytic reduction of the various nitroalkanes as a function of concentration.

2.5.6.2 Catalytic efficiency versus scan rate:

As described above, the catalytic efficiency tends to decrease with an increase in the scan rate. The reason being the time scale for the reaction tends to decrease with the scan rate resulting in the decrease in the number of catalytic turnovers.

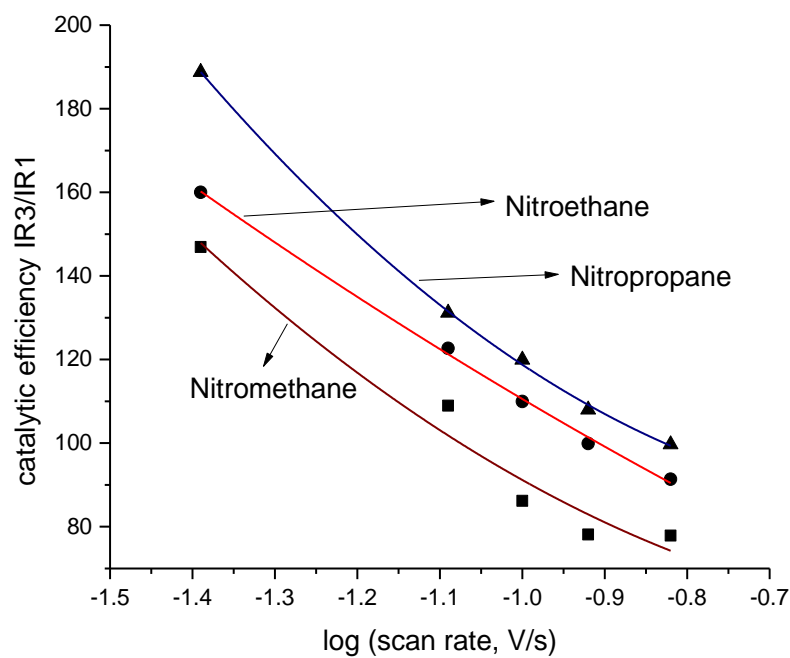


Figure 2.11 Catalytic efficiencies of iNOSoxy-mediated reduction of the various nitroalkanes as a function of scan rate

2.5.7 Redox properties of eNOSoxy in surfactant films on PG electrodes and eNOSoxy-mediated catalytic reduction of nitromethane

Like in the iNOSoxy case, surfactant film ddab was employed in the immobilization of eNOSoxy on the surface of the electrode. [45]. A typical voltammogram of eNOSoxy is shown in Figure 2.12. We observe two redox couples: the first redox couple (R_1/O_1) is assigned to the reversible reduction of Fe^{III} to Fe^{II} of the heme center (Equation 3), and the next couple (R_2/O_2) is assigned to the reduction of Fe^{II} to a formal “ Fe^I ” (Equation 4)



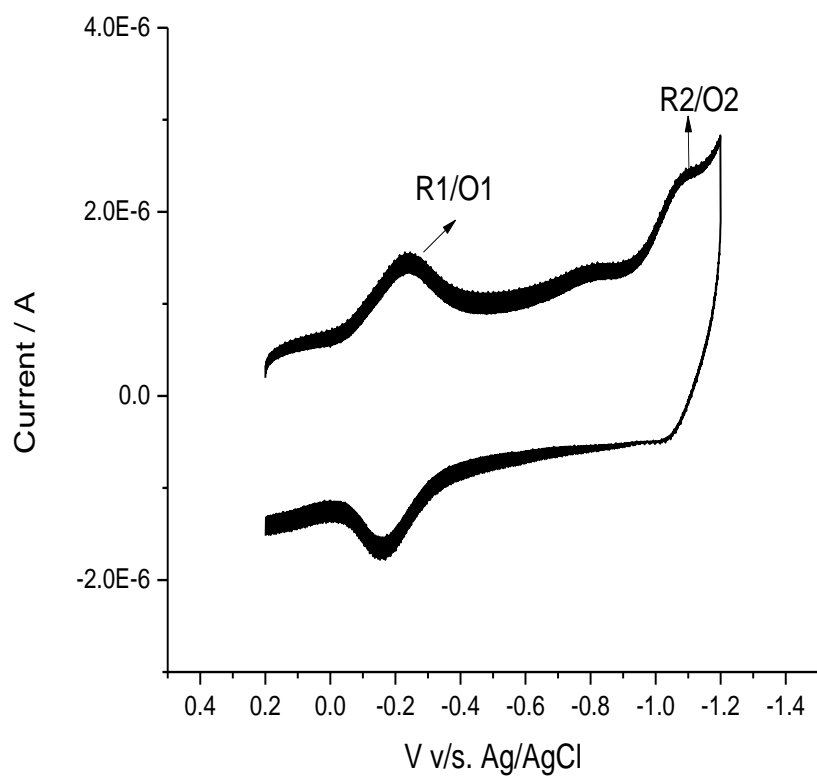


Figure 2.12 Cyclic voltammetry of eNOSoxy/ddab/PG at pH 5.5 in acetate buffer at scan rate 0.1V/s.

2.5.7.1 Electrocatalytic reduction of nitromethane on eNOSoxy/ddab/PG:

Similar to the iNOSoxy case, the presence of nitromethane at the eNOSoxy/ddab/PG electrode gives rise to an irreversible peak, R_3 at -1.0 V vs. Ag/AgCl in parallel with the disappearance of the the Fe^{II}/Fe^I redox couple[54].

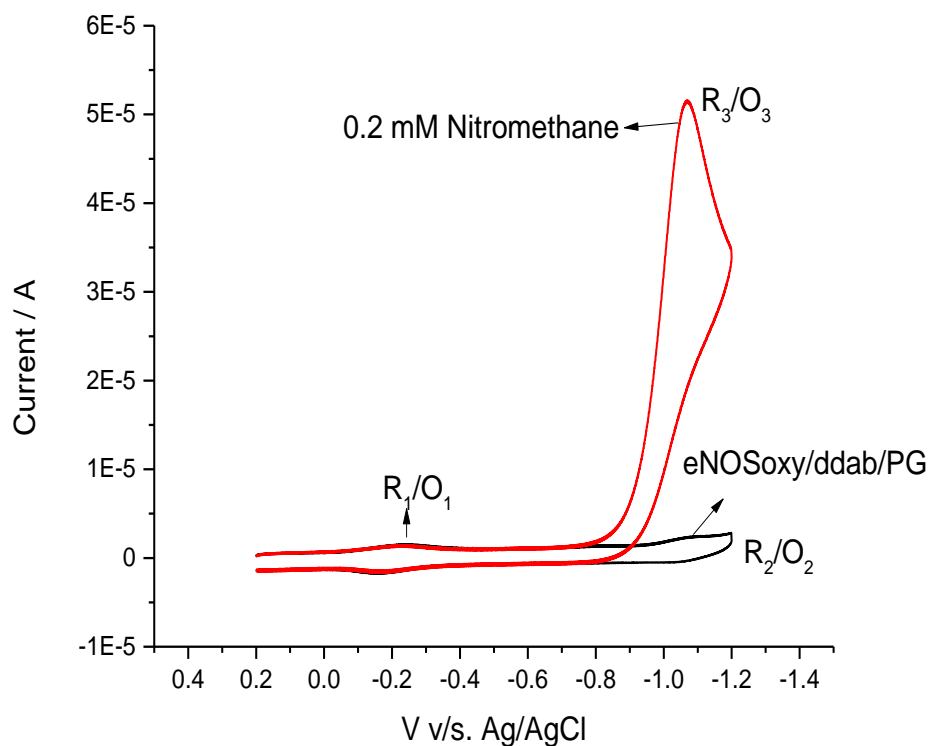


Figure 2.13 Cyclic voltammetry of eNOSoxy in ddab on PG electrode in absence and presence of nitromethane.

2.5.7.2 Effect of nitromethane concentration on eNOSoxy-mediated catalytic reduction

As the concentration of the nitromethane added increases, there is an observed increase in the catalytic wave R_3 . The catalytic efficiency initially increases and then curves down with a shape typical of enzyme saturation kinetics.

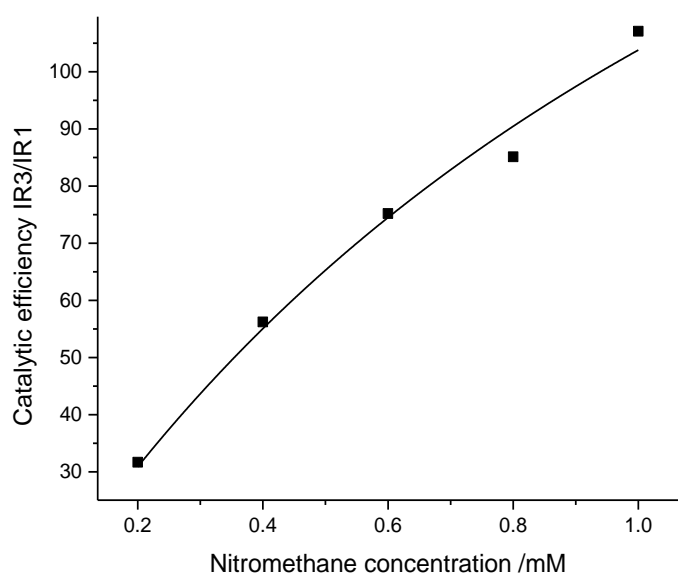


Figure 2.14 Comparison of catalytic efficiencies as a function of nitromethane concentrations in acetate buffer at pH 5.5

2.5.7.3 Comparison of the effect of different nitroalkanes on the catalytic efficiencies of eNOSoxy:

All the nitroalkanes in our study show that the catalytic efficiency initially increases and then, tends to curve down with a shape typical of enzyme saturation kinetics. Such behavior was described by using the Michaelis-Menten model.

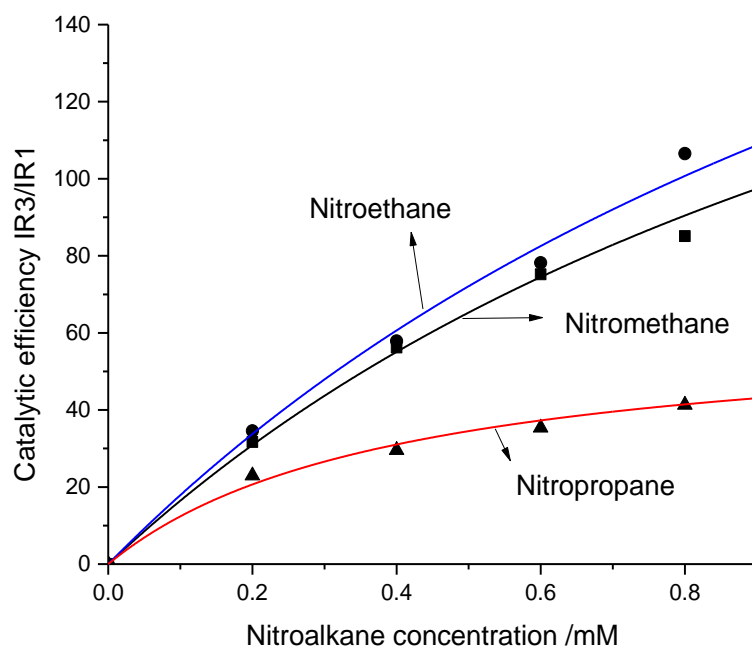


Figure 2.15 Catalytic efficiency of eNOSoxy-mediated catalytic reduction of the various nitroalkanes as a function of concentration.

2.5.8. Comparison of catalytic efficiencies of iNOSoxy- and eNOSoxy-mediated catalytic reduction for the various nitroalkanes:

2.5.8.1 Comparison of the effect of different nitroalkanes on the catalytic efficiencies of iNOSoxy and eNOSoxy

As we explained in the case of iNOSoxy, the peak area of the $\text{Fe}^{3+}/\text{Fe}^{2+}$ reversible reduction is proportional to the amount of electroactive species in the film. The surface concentration of active iNOSoxy or eNOSoxy on electrodes will be different. This difference in surface concentrations can be a problem when comparing the catalytic currents for different catalysts but this can be corrected by knowing the average catalyst surface concentration using the charge integration procedure for a typical electrode under the same conditions. As we will see later in section 2.5.9, the exact amount of NOSoxy catalyst on the surface of the electrode is an important quantity in order to fit the experimental points of a each case using the Michaelis-Menten framework. For comparison purposes, however, the normalized current ratio of R3/R1 can be used to compare the catalytic turnover of eNOSoxy and iNOSoxy for a given nitroalkane despite the difference in the absolute amounts of NOSoxy catalyst on the surface of the electrode. Figure 2.16 shows the case of nitropropane's catalytic reduction by iNOSoxy and eNOSoxy, which shows relatively higher catalytic turnovers for iNOSoxy compared to eNOSoxy.

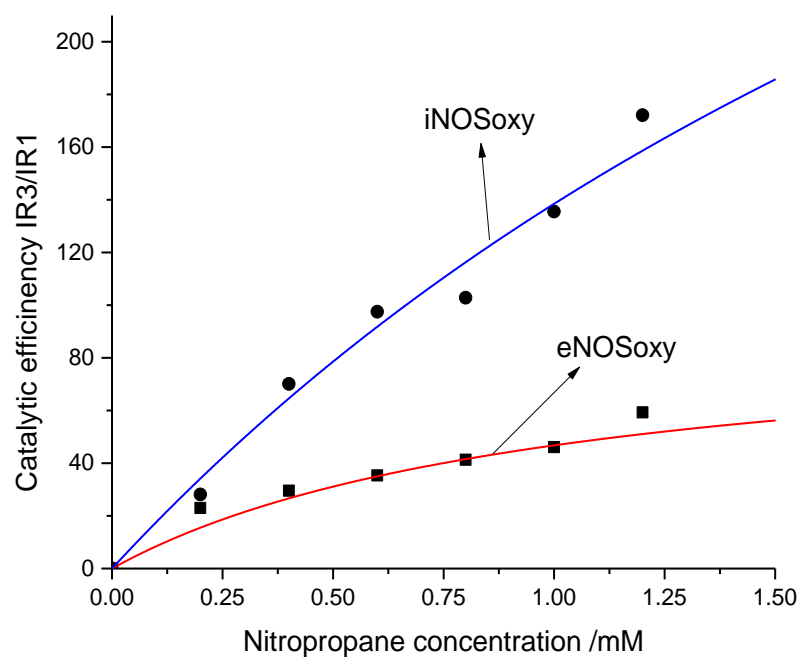


Figure 2.16 Comparison of the catalytic efficiencies of iNOSoxy and eNOSoxy as a function of nitropropane concentrations in acetate buffer at pH 5.5.

2.5.8.2 Comparison of the catalytic efficiency as function of scan rate for eNOSoxy- with iNOSoxy-mediated reduction of nitroalkanes

We compared the catalytic efficiency of iNOSoxy- and eNOSoxy-mediated reduction of nitromethane at the same concentrations as a function of scan rate. As expected, the catalytic efficiency, defined by the ratio (I_{R3}/I_{R1}) is larger at smaller scan rates and gradually drops as the scan rate increases for both iNOSoxy and eNOSoxy (Figures 2.17, 2.18 and 2.19). However, eNOSoxy shows lower catalytic efficiencies when compared to iNOSoxy for all nitroalkanes considered for our study (Figures 2.17, 2.18 and 2.19). The reasons for the differences could be due to the structural differences in iNOSoxy and eNOSoxy, which we will discuss in section 3.4.

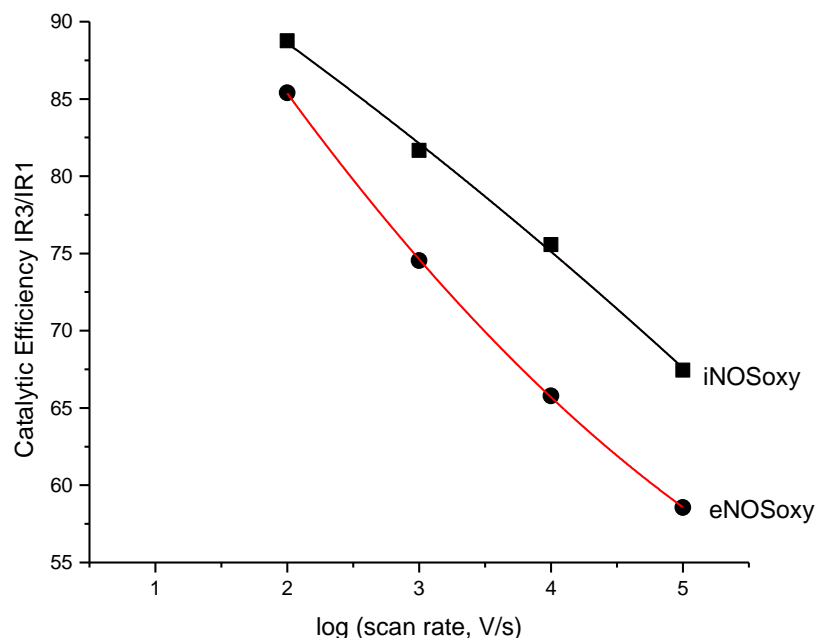


Figure 2.17 Catalytic efficiencies of iNOSoxy and eNOSoxy-mediated reduction at 0.8 mM nitromethane as a function of scan rate in V/s

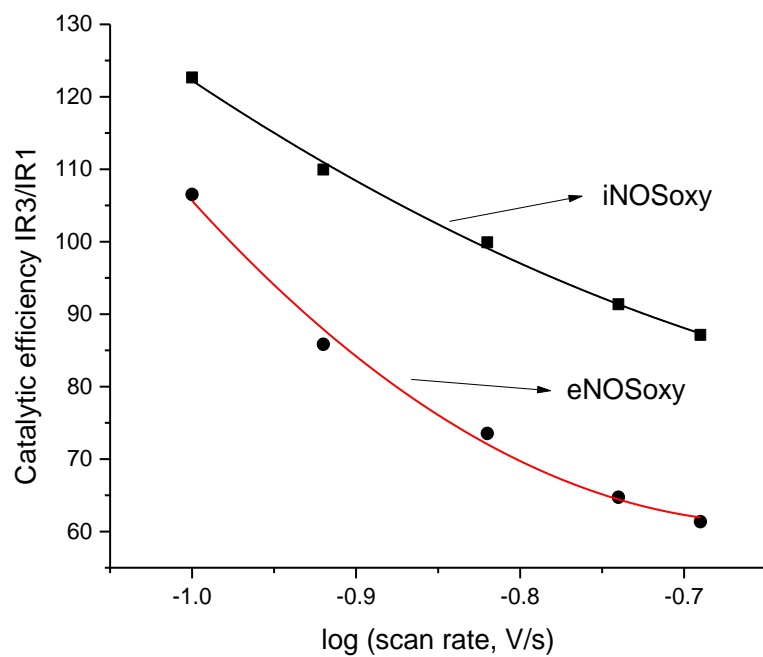


Figure 2.18 Catalytic efficiencies of iNOSoxy and eNOSoxy-mediated reduction at 0.8 mM nitroethane as a function of scan rate in V/s

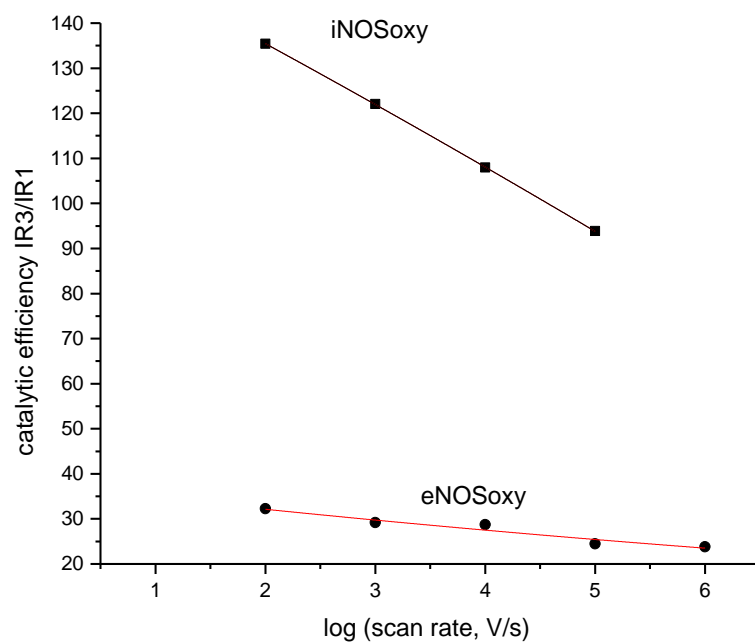


Figure 2.19 Catalytic efficiencies of iNOSoxy and eNOSoxy-mediated reduction at 0.8 mM nitropropane as a function of scan rate in V/s

2.5.9 Michaelis Menten Kinetics:

The plot obtained by comparing catalytic efficiencies at different concentrations of nitroalkanes is in essence a plot of enzymatic rates as function of concentration and could be fit to Michaelis Menten equation (Equation 5),

$$V = \frac{V_{\max} \cdot [S]}{K_m + [S]} \quad (\text{Michaelis Menten equation}) \quad (5)$$

K_m represents the constant for the formation of enzyme substrate complex. K_m is equal to the substrate concentration at which the reaction rate is half its maximum value. The value of K_m for an enzyme depends on the particular substrate. The k_{cat} value gives the turnover number, i.e. the number of molecules of the substrate that each enzyme molecule converts in a unit time. The higher the k_{cat} value the more efficient the enzyme is for the catalytic transformation under consideration. Fitting the curve of catalytic efficiency (equivalent to the rate of enzymatic reaction) versus substrate concentration to the electrochemical form of the Michaelis-Menten model allows us to extract the k_{cat} and K_m values.

By measuring the currents of the iNOSoxy- and eNOSoxy-mediated catalytic reduction of nitroalkanes and extracting enzymatic reaction parameters such as K_m and k_{cat} , we will be able to compare and contrast the catalytic behavior of iNOSoxy and eNOSoxy towards the nitroalkanes. The catalytic current at the NOS-modified electrode in the presence of nitroalkanes is a measure of the rate of catalytic reduction and can be used in an equation equivalent to the general Michaelis-Menten equation in solution.

The Michaelis-Menten equation (Equation 6) using catalytic currents at the electrode is of the form:

$$I_{cat} = \frac{nFA\Gamma k_{cat} [s]}{K_m + [s]} \quad (6)$$

In this case, I_{cat} is the catalytic current at the peak R_3 .

‘n’ being the number of electrons in the reaction.

‘F’ is the Faraday constant.

‘A’ is the area of the electrode.

‘ Γ ’ is the surface concentration of the enzyme, which we determine by integrating the peak current at R_1 .

The surface concentration of the enzyme is required to calculate the K_m and k_{cat} values of the enzyme in the presence of different nitroalkanes. The surface concentration of the enzyme is determined by integration of the reduction current as shown in Figure 2.20 and Figure 2.21 at the R_1 peak where the Fe^{III} to Fe^{II} conversion takes place. The area under the voltammogram is a measure of the charge passed during the reduction of all accessible $Fe(III)$ sites in the film. The charge passed is a measure of the number of electrons transferred, and thus the number of iNOSoxy molecules present given the one heme per iNOSoxy protein relationship. To this end, the voltammogram is obtained at a scan rate as low as 5 mV/sec [30], which allows for the reduction of the total electroactive protein in the film. The average surface concentration of the electroactive iNOSoxy estimated indicates that only a small percentage of the total amount of iNOSoxy deposited on the electrode surface was actually electrochemically reduced. This may suggest that only those iNOSoxy molecules in the inner layers of the film closest to the surface of the electrode and with a suitable orientation exchange electrons with the electrode and contribute to the observed redox reaction [55].

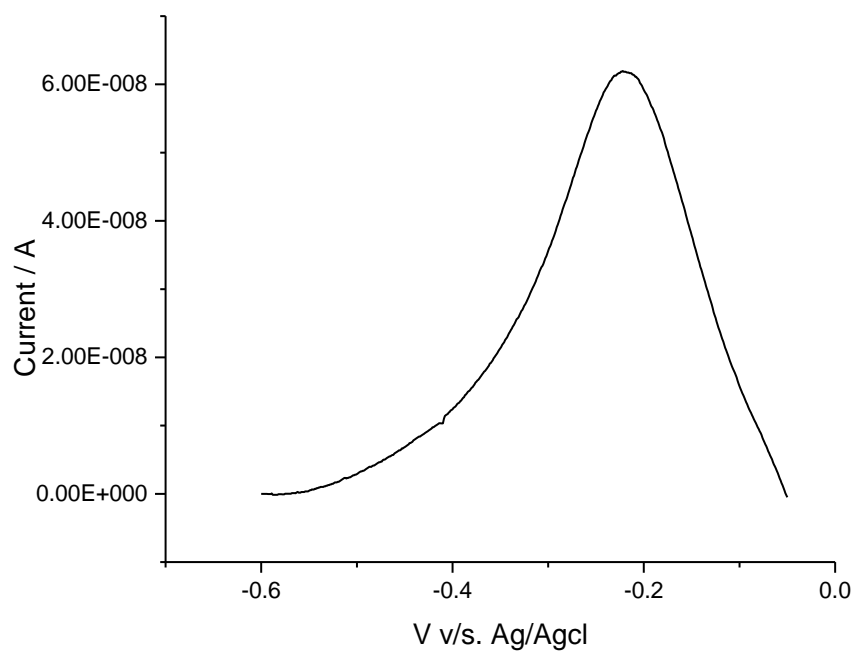


Figure 2.20 Integration of iNOSoxy at the Fe³⁺/Fe²⁺ redox couple; area under the curve is a measure of the charge passed

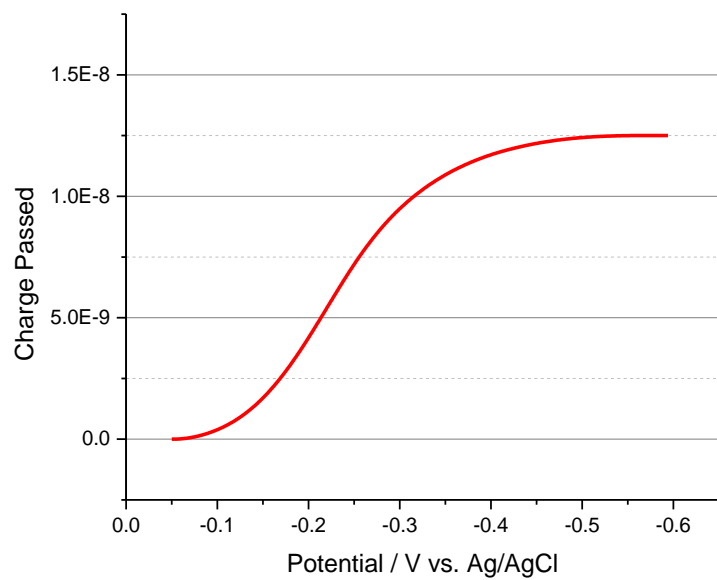


Figure 2.21 Integration of the area under the voltammogram at R1 of iNOSoxy/ddab/PG taken at 5mV/s

The K_m values were extracted from the plots of catalytic efficiencies as function of concentration of nitroalkanes through nonlinear fitting using the Michaelis-Menten model (equation 6).

Figure 2.22 shows the fitting of turnovers of iNOSoxy-mediated catalytic reduction as a function of concentration for the three nitroalkanes. The K_m values of obtained are listed in Table 2.1. Figure 2.23 shows the fitting results in the case of eNOSoxy-mediated catalytic reduction. The corresponding K_m values are also listed in Table 2.1.

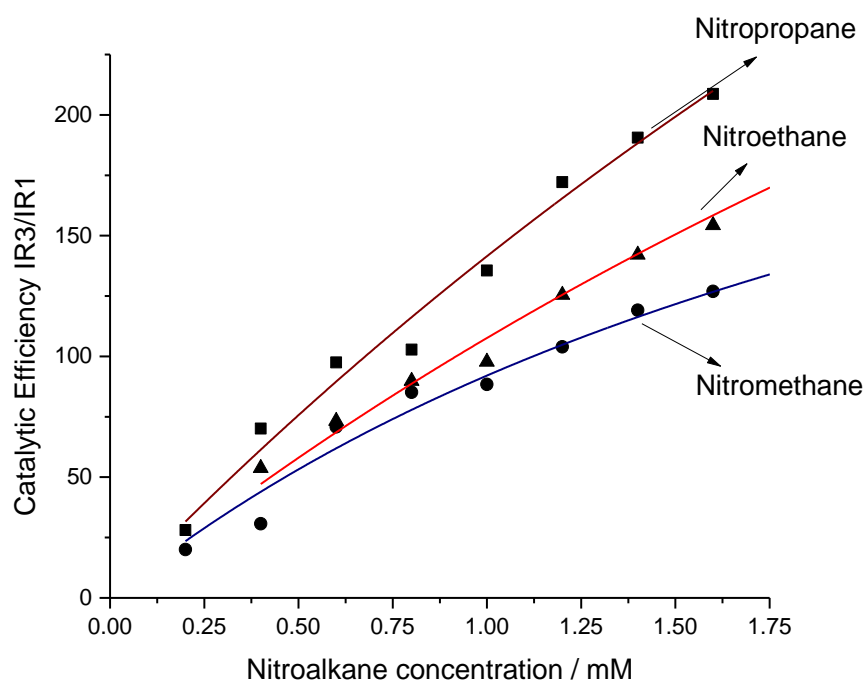


Figure 2.22 Catalytic efficiency of iNOSoxy-mediated catalytic reduction of the various nitroalkanes as a function of concentration to obtain the K_m values.

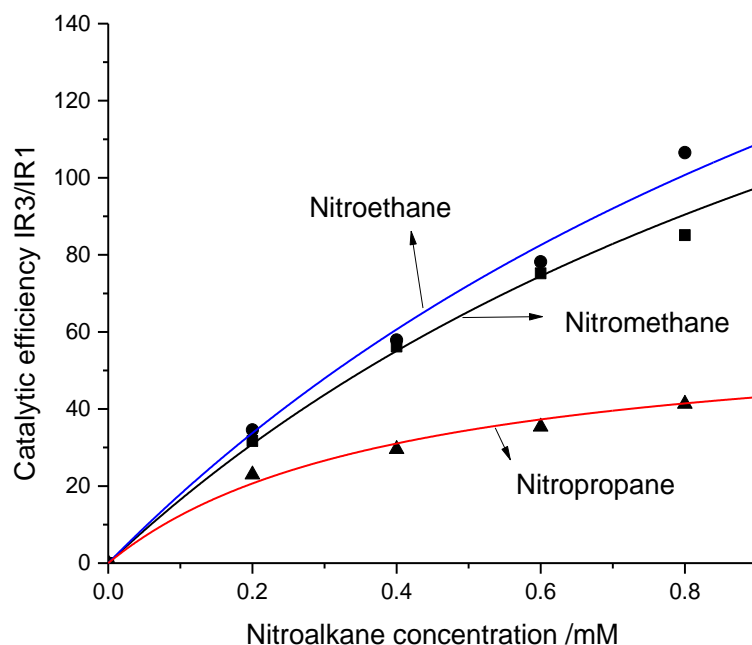


Figure 2.23 Catalytic efficiency of eNOSoxy-mediated catalytic reduction of the various nitroalkanes as a function of concentration to obtain the K_m values.

Table 2.1 The K_m Values for iNOSoxy and eNOSoxy in the presence of nitroalkanes

Nitroalkane	K_m iNOSoxy (mM)	K_m eNOSoxy (mM)
Nitromethane	2.9 ± 1.4	1.44 ± 0.37
Nitroethane	4.075 ± 2.0	1.56 ± 0.45
Nitropropane	6.919 ± 2.9	0.40 ± 0.09

As stated before, K_m is a measure of the substrate concentration at which the catalytic reaction rate is half of its maximum value. The above results show that K_m values of iNOSoxy are generally higher than the K_m values obtained for eNOSoxy,

indicating that the binding affinity of the nitroalkanes to the active form of eNOSoxy is higher than with iNOSoxy.

CHAPTER III

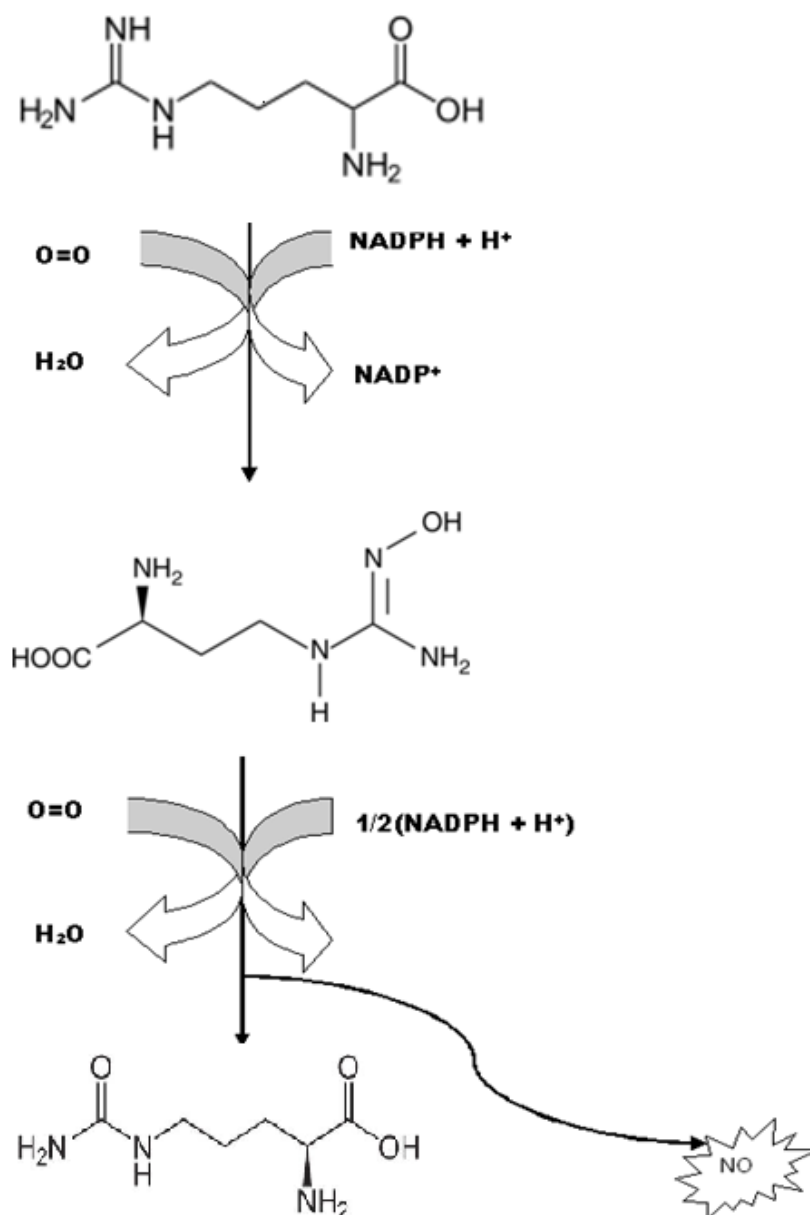
EFFECT OF NITROALKANES ON THE CATALYTIC SYNTHESIS

OF NITRIC OXIDE (NO) BY iNOS_{oxy}

3.1. Introduction:

Nitric Oxide (NO) is produced by nitric oxide synthase (NOS) enzymes from the substrate, L-arginine (Arg). NOSs are enzymes that catalyze a two step reaction to form citrulline and nitric oxide (NO) from L-Arg. The NO synthesis is complicated because the catalytic assembly involves a variety of co-factors[56]. The biosynthetic reaction consumes 1.5 NADPH molecules and two atoms of oxygen for the synthesis of NO. The calmodulin (CaM) binding is needed for function and triggers inter-domain electron transfer between the reduced FMN and the heme group. NADPH is the source of reducing equivalents in the reaction.. During the catalytic cycle, electrons are transferred from the NADPH at its binding site to the heme through FAD and FMN. A pterin cofactor (tetrahydrobiopterin, H₄B) is involved and has multiple functions during the catalytic cycle. It promotes dimer assembly of iNOS heme-containing monomer, increases the arginine binding affinity, modifies heme midpoint potential and induces a high spin shift of the heme iron. The H₄B ring also makes π -stacking and hydrogen-bonding interactions with several conserved residues that are provided by both subunits

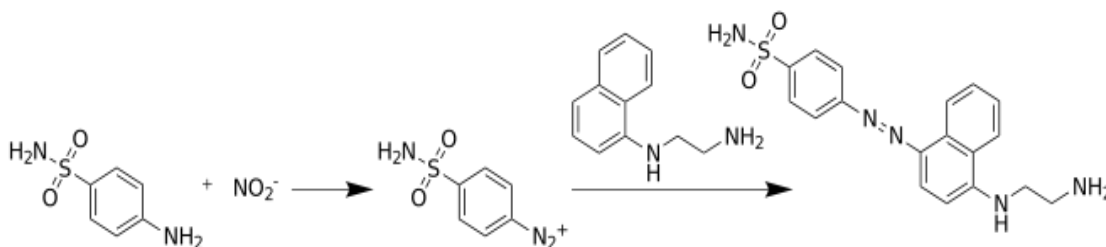
of the NOSoxy dimer[57] . Although we can follow the two-step reaction using the full-length enzyme, one can study the second step only on iNOSoxy or eNOSoxy using N-hydroxyarginine (NOHA) intermediate as the substrate. Reducing equivalents are provided in the form of hydrogen peroxide (H_2O_2), which is used to trigger the catalytic reaction.



Scheme 3.1 Nitric Oxide Biosynthesis

In this chapter, we compared the native enzymatic activity of NOSs (in the form of iNOSoxy and eNOSoxy) in the presence of varying concentrations of nitroalkanes (nitromethane, nitroethane, and nitropropane). Nitric oxide synthase activity can be assayed by either measuring the citrulline or NO itself. Formation of tritium- or ^{14}C -labelled citrulline from labeled L-arginine is one of the methods[34]. Another straightforward method, which is widely used, is to measure stable end-products of NO in aqueous solutions, namely nitrite (NO_2^-) and nitrate (NO_3^-). The reduction of NO_3^- to NO_2^- followed by the colorimetric Griess reaction to measure NO_2^- provides a quantitative measure of NO synthesis, and thus the catalytic activity of NOS or NOSoxy enzymes could be measured.

All the ingredients for the NOS reaction (substrate NOHA in our case, and the H_4B cofactor) are added to the reaction mixture. The reaction is triggered by adding H_2O_2 and stopped after a desired amount of time by adding glacial acetic acid and transferring the reaction tube to ice-water. The nitric oxide product (NO) in the form of nitrite (NO_2^-) is quantified using the Griess assay as described in Scheme 3.2 below [21]. The Griess assay determines the amount of nitrite (NO_2^-) in the reaction mixture spectrophotometrically through the quantification of a stable pink color diazo compound.



Scheme 3.2 Griess Assay

The amount of nitrite formed is essentially equal to the amount of NO produced in the reaction mixture. Thus, the amount of nitrite (NO_2^-) formed can be used to

measure the enzyme activity of iNOSoxy or eNOSoxy in terms of NO synthesis from NOHA.

3.2 The Griess assay

The activity of an enzyme is the number of moles of the substrate converted to product in a unit time. In this method, all the reaction ingredient needed for the formation of NO (NOHA, H₄B), were incubated with iNOSoxy or eNOSoxy in the reaction mixture. H₂O₂ was used to start the reaction and catalase was added to stop the reaction. The reaction tube is immediately transferred to ice and stored there until analysis by the Griess assay. Sulfanilamide and NED is used for the formation of the colored azo compound which was quantified by using uv-vis[21]. The typical specific activity of iNOSoxy samples in the absence of nitroalkanes was found out to be 63.5 nmol(NO).min⁻¹.nmol (enzyme)⁻¹

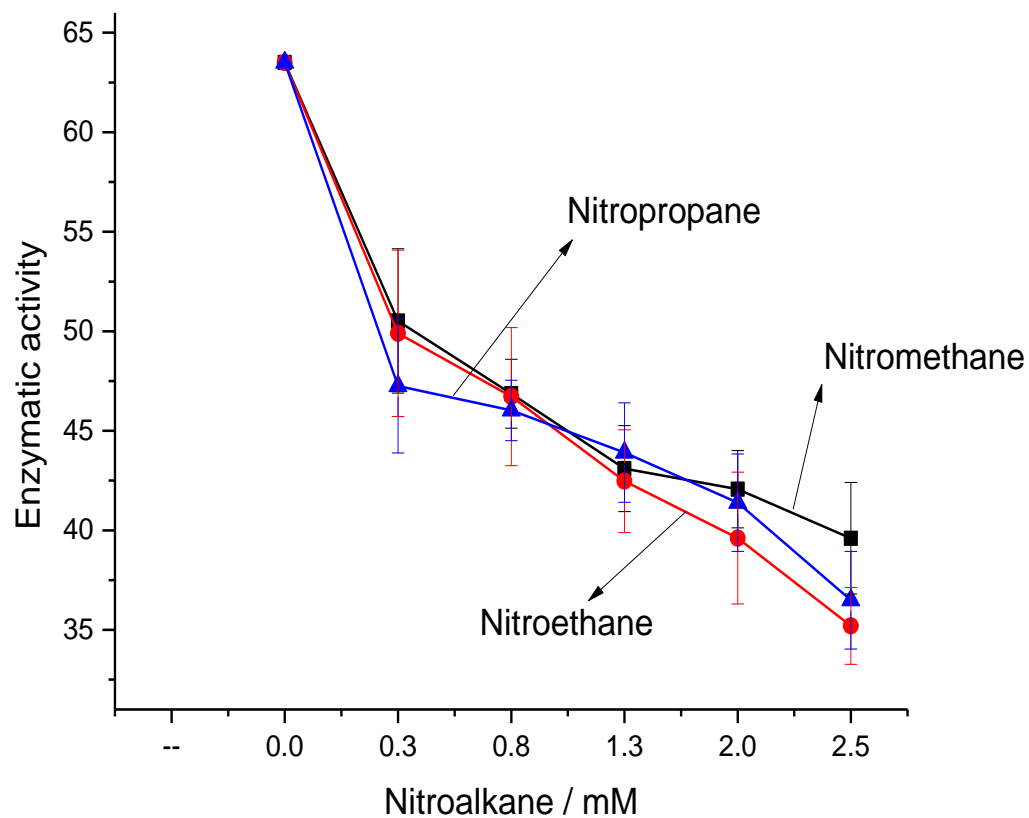


Figure 3.1 Comparison of iNOSoxy activity (NO synthesis) in the presence of nitromethane (black solid squares), nitroethane (red solid circles), and nitropropane (blue solid triangles) at various concentration levels. Data are averages of three trials. Bars represent standard deviations

3.3 Results:

Figure 3.1 shows that NO synthesis activity of iNOSoxy decreases with all nitroalkanes in a dose-response manner. While the overall activity of eNOSoxy is typically lower than iNOSoxy, similar trends were obtained with eNOSoxy where the activity decreases with increase in concentration indicating that the eNOSoxy is being inhibited by the nitroalkanes. Figure 3.2 shows the effect of nitromethane addition on eNOSoxy enzymatic NO synthesis.

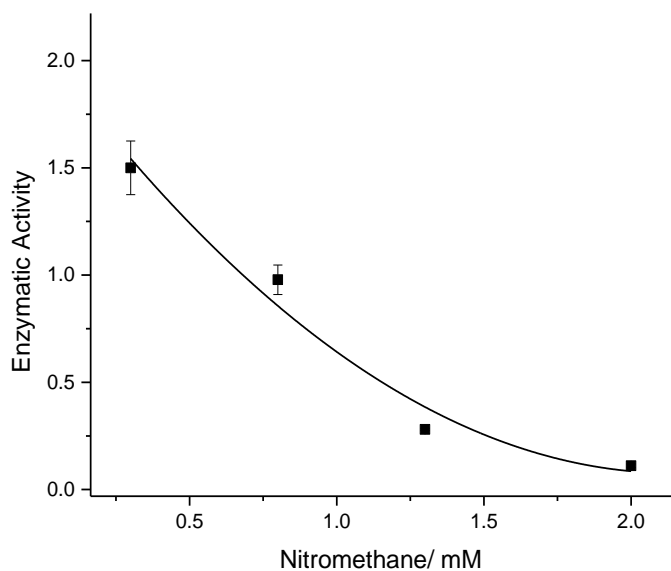


Figure 3.2 Comparison of eNOSoxy activity (NO synthesis) in the presence of nitromethane (black solid squares). Data are averages of three trials. Bars represent standard deviations

Overall, nitromethane, like other nitroalkanes, seems to inhibit iNOSoxy and eNOSoxy by interacting with one or more active forms of the enzyme during catalytic turnover.

We focused on nitromethane to closely compare the effect on eNOSoxy and iNOSoxy in terms of NO synthesis activities. The absolute activities of eNOSoxy and iNOSoxy are significantly different. We therefore normalized the activities at various nitromethane concentrations to the enzyme activity found in the absence of nitromethane. Figure 3.3 shows that the normalized activity for both iNOSoxy and eNOSoxy decreases as the concentration of nitromethane increases. However, eNOSoxy shows a greater relative shutdown of activity compared to iNOSoxy as nitromethane concentration increases. The figure shows that nitromethane causes a larger degree of inhibition of enzyme activity of eNOSoxy as compared to iNOSoxy.

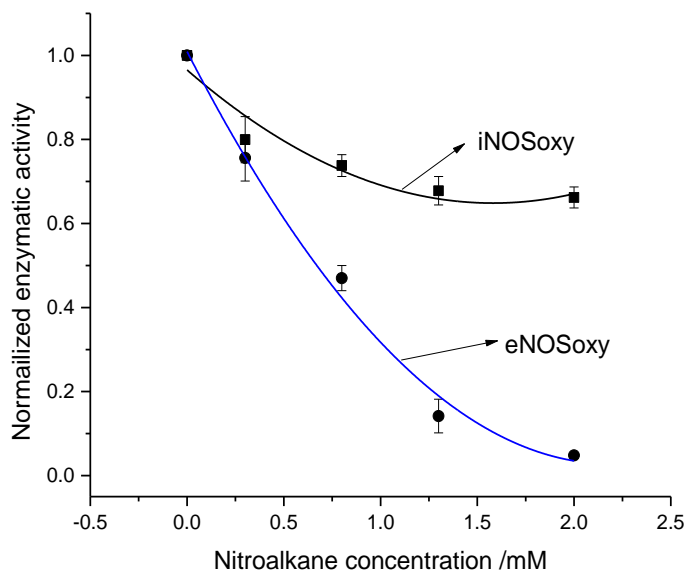


Figure 3.3 Comparison of the normalized enzyme activity of iNOSoxy (black solid squares) with eNOSoxy (black solid circles) in the presence of nitromethane. Data are average of three trials. Bars represent standard deviations

CORRELATION OF NOSoxy-MEDIATED CATALYTIC REDUCTION OF NITROALKANES AND OBSERVED INHIBITION OF NOS REACTION

Our results show that iNOSoxy and eNOSoxy mediate the electrocatalytic reduction of simple nitroalkanes used in this investigation; namely, nitromethane, nitroethane, and nitropropane. We compared and contrasted electrocatalytic responses of iNOSoxy- and eNOSoxy-modified electrodes in the presence of the various nitroalkanes using the cyclic voltammetry. Both enzyme isoforms (iNOSoxy and eNOSoxy) exhibit typical saturation kinetics as the concentration of substrates is increased. We found that the K_m values of iNOSoxy are higher than those of eNOSoxy, indicating a higher binding affinity of the nitroalkanes to the active form of eNOSoxy as compared to iNOSoxy during catalytic reduction.

On a related front, we examined if the binding interaction of nitroalkanes with active forms of eNOSoxy and iNOSoxy as implied from the electrocatalytic reductions of nitroalkanes on NOSoxy-modified electrodes correlate with the NOS reaction inhibition in the presence of the same nitroalkanes. We found that nitric oxide synthesis as catalyzed by iNOSoxy and eNOSoxy is significantly affected in the presence of nitroalkanes. The degree of inhibition is higher as the concentration of nitroalkane increases. Interestingly, we found that nitromethane catalytic reduction by eNOSoxy shows a lower K_m value compared to the iNOSoxy case. In parallel, we show that the inhibitory effect of nitromethane on the NOS reaction by eNOSoxy is more drastic than its effect on the NOS reaction by iNOSoxy. While the underlying reason for this differential effect on iNOSoxy and eNOSoxy is not clearly known at this time, the correlation of K_m values of the NOSoxy-mediated catalytic reduction of nitromethane and its inhibitory effect on the NOS reaction may find an explanation in structural differences of eNOSoxy and iNOSoxy. The distinct effects of nitromethane on catalytic activities of eNOSoxy and iNOSoxy may be attributed to the environment around the heme group in the two isoforms; however, early structural studies established that the heme active site is highly conserved in iNOSoxy and eNOSoxy [58]. In general, NOS isozymes show a 60 to 70 % homology. Despite the near identical active site structure of

NOS isoforms, a number of structure-based NOS inhibitors have been reported, which capitalize on distinct features at or near the active site. These features include amino acid changes, differential effects of induced conformational changes, or distinct changes in steric crowding, to cite a few [59] [60] [61] [62]. The simple nitroalkanes used in this work, including nitromethane, are small organic molecules and are not expected to benefit from the interactions reported for bulkier NOS inhibitors. However, distinct features such as the access gate to the active site of iNOS_{oxy} versus eNOS_{oxy}, or the nature of select amino acids lining their access channel, may affect the extent of access of nitromethane and its exposure to the heme active site from the solution bulk. In terms of differential access, previous reports have invoked the narrower substrate access channel in iNOS as compared to eNOS as one factor among many that rationalize the poor inhibitory potency of select nitroarginine-based dipeptides[59]. The active site of eNOS itself is larger than that of iNOS [63]. While the situation may be different in the case of the small nitroalkanes used here, the relatively wider access channel to the heme active site in eNOS_{oxy} as compared to iNOS_{oxy} is expected to result in a higher exposure of the heme catalytic site to the small nitroalkane molecules, which would translate to a relative higher degree of inhibition of the catalytic activity of eNOS_{oxy} versus iNOS_{oxy}. Also, the nitro group of nitromethane and other nitroalkanes used in this work is expected to dynamically interact with residues in the access channel and at the active site. This electron-withdrawing group on bulkier inhibitors is known to hydrogen bond to nearby amide nitrogens as well as to side chain heteroatoms. The relatively narrow channel and small active site of iNOS versus eNOS, in concert with few non-conserved residues (e.g. Phe 475 in eNOS versus Tyr 486 in iNOS; Ser 356 in eNOS versus Asn 367 in iNOS; Ala 448 in eNOS versus Ile 459 in iNOS) and their expected distinct dynamic electrostatic interaction with the nitro group of nitromethane may also explain the larger effect on eNOS catalysis. The same structural considerations may explain the correlated *K_m* values observed by cyclic voltammetry for eNOS_{oxy}- and iNOS-_{oxy} mediated catalytic reduction of nitroalkanes on NOS_{oxy}-modified pyrolytic graphite electrodes.

REFERENCES

1. Boutros, J. and M. Bayachou, *Myoglobin as an efficient electrocatalyst for nitromethane reduction*. Inorg Chem, 2004. **43**(13): p. 3847-53.
2. Sakano, K., et al., *Mechanism of metal-mediated DNA damage induced by a metabolite of carcinogenic acetamide*. Chem Biol Interact, 2004. **149**(1): p. 52-9.
3. Lewis, T.R., C.E. Ulrich, and W.M. Busey, *Subchronic inhalation toxicity of nitromethane and 2-nitropropane*. J Environ Pathol Toxicol, 1979. **2**(5): p. 233-49.
4. Kappers, W.A., et al., *Comparison of three different in vitro mutation assays used for the investigation of cytochrome P450-mediated mutagenicity of nitro-polycyclic aromatic hydrocarbons*. Mutat Res, 2000. **466**(2): p. 143-59.
5. Goggelmann, W., et al., *Genotoxicity of 2-nitropropane and 1-nitropropane in Salmonella typhimurium and human lymphocytes*. Mutagenesis, 1988. **3**(2): p. 137-40.
6. Murray, G.I., *The role of cytochrome P450 in tumour development and progression and its potential in therapy*. J Pathol, 2000. **192**(4): p. 419-26.
7. Page, E.H., et al., *Peripheral neuropathy in workers exposed to nitromethane*. Am J Ind Med, 2001. **40**(1): p. 107-13.
8. Omura, T., *Forty years of cytochrome P450*. Biochem Biophys Res Commun, 1999. **266**(3): p. 690-8.
9. Park, J.E., et al., *Contribution of cytochrome P450 3A4 and 3A5 to the metabolism of atorvastatin*. Xenobiotica, 2008. **38**(9): p. 1240-51.
10. Conaway, C.C., et al., *Comparison of oxidative damage to rat liver DNA and RNA by primary nitroalkanes, secondary nitroalkanes, cyclopentanone oxime, and related compounds*. Cancer Res, 1991. **51**(12): p. 3143-7.
11. Harada, N. and T. Omura, *Participation of cytochrome P-450 in the reduction of nitro compounds by rat liver microsomes*. J Biochem, 1980. **87**(5): p. 1539-54.
12. Jakoby, W.B. and D.M. Ziegler, *The enzymes of detoxication*. J Biol Chem, 1990. **265**(34): p. 20715-8.
13. Zhang, Z. and J.F. Rusling, *Electron transfer between myoglobin and electrodes in thin films of phosphatidylcholines and dihexadecylphosphate*. Biophys Chem, 1997. **63**(2-3): p. 133-46.
14. Fantuzzi, A., M. Fairhead, and G. Gilardi, *Direct electrochemistry of immobilized human cytochrome P450 2E1*. J Am Chem Soc, 2004. **126**(16): p. 5040-1.
15. Hagen, K.D., et al., *Electrochemistry of mammalian cytochrome P450 2B4 indicates tunable thermodynamic parameters in surfactant films*. J Inorg Biochem. **129**: p. 30-4.
16. Udit, A.K., M.G. Hill, and H.B. Gray, *Electrochemistry of cytochrome P450 BM3 in sodium dodecyl sulfate films*. Langmuir, 2006. **22**(25): p. 10854-7.
17. Sultana, N., J.B. Schenkman, and J.F. Rusling, *Protein film electrochemistry of microsomes genetically enriched in human cytochrome p450 monooxygenases*. J Am Chem Soc, 2005. **127**(39): p. 13460-1.
18. Stuehr, D.J., et al., *Purification and characterization of the cytokine-induced macrophage nitric oxide synthase: an FAD- and FMN-containing flavoprotein*. Proc Natl Acad Sci U S A, 1991. **88**(17): p. 7773-7.

19. Samer, C.F., et al., *Applications of CYP450 testing in the clinical setting*. Mol Diagn Ther. **17**(3): p. 165-84.
20. Dirsch, V.M., H. Stuppner, and A.M. Vollmar, *The Griess assay: suitable for a bio-guided fractionation of anti-inflammatory plant extracts?* Planta Med, 1998. **64**(5): p. 423-6.
21. Miranda, K.M., M.G. Espey, and D.A. Wink, *A rapid, simple spectrophotometric method for simultaneous detection of nitrate and nitrite*. Nitric Oxide, 2001. **5**(1): p. 62-71.
22. Teodorescu, M., *Calorimetric study of the selected nitroalkane+chloroalkane binary systems*. J Therm Anal Calorim, 2013. **10**.
23. Gildner, P.G., et al., *Benzylation of nitroalkanes using copper-catalyzed thermal redox catalysis: toward the facile C-alkylation of nitroalkanes*. J Am Chem Soc. **134**(24): p. 9942-5.
24. Shepherd, G., J. Grover, and W. Klein-Schwartz, *Prolonged formation of methemoglobin following nitroethane ingestion*. J Toxicol Clin Toxicol, 1998. **36**(6): p. 613-6.
25. Jiang, Y., et al., *The detection of cytochrome P450 2E1 and its catalytic activity in rat testis*. Biochem Biophys Res Commun, 1998. **246**(3): p. 578-83.
26. Shenfield, G.M., *Genetic polymorphisms, drug metabolism and drug concentrations*. Clin Biochem Rev, 2004. **25**(4): p. 203-6.
27. Sevrioukova, I.F. and T.L. Poulos, *Structural and mechanistic insights into the interaction of cytochrome P4503A4 with bromoergocryptine, a type I ligand*. J Biol Chem. **287**(5): p. 3510-7.
28. Hruby, K. and P. Anzenbacher, *[Cytochrome P450--its significance in the biotransformation of xenobiotics and interspecies comparisons]*. Cesk Fysiol, 1997. **46**(1): p. 34-9.
29. Rendic, S. and F.J. Di Carlo, *Human cytochrome P450 enzymes: a status report summarizing their reactions, substrates, inducers, and inhibitors*. Drug Metab Rev, 1997. **29**(1-2): p. 413-580.
30. Guengerich, F.P., *Common and uncommon cytochrome P450 reactions related to metabolism and chemical toxicity*. Chem Res Toxicol, 2001. **14**(6): p. 611-50.
31. Anzenbacher, P. and E. Anzenbacherova, *Cytochromes P450 and metabolism of xenobiotics*. Cell Mol Life Sci, 2001. **58**(5-6): p. 737-47.
32. Goepfert, A.R., H. Scheerens, and N.P. Vermeulen, *Oxygen and xenobiotic reductase activities of cytochrome P450*. Crit Rev Toxicol, 1995. **25**(1): p. 25-65.
33. Alderton, W.K., C.E. Cooper, and R.G. Knowles, *Nitric oxide synthases: structure, function and inhibition*. Biochem J, 2001. **357**(Pt 3): p. 593-615.
34. Knowles, R.G. and S. Moncada, *Nitric oxide synthases in mammals*. Biochem J, 1994. **298 (Pt 2)**: p. 249-58.
35. Gorren, A.C. and B. Mayer, *The versatile and complex enzymology of nitric oxide synthase*. Biochemistry (Mosc), 1998. **63**(7): p. 734-43.
36. Stuehr, D.J., *Mammalian nitric oxide synthases*. Biochim Biophys Acta, 1999. **1411**(2-3): p. 217-30.
37. Andrew, P.J. and B. Mayer, *Enzymatic function of nitric oxide synthases*. Cardiovasc Res, 1999. **43**(3): p. 521-31.
38. Marletta, M.A., *Nitric oxide synthase: aspects concerning structure and catalysis*. Cell, 1994. **78**(6): p. 927-30.

39. Klingenberg, M., *Pigments of rat liver microsomes*. Arch Biochem Biophys, 2003. **409**(1): p. 2-6.
40. Agency, U.S.E.P., *Health and Environmental Effects Profile for 2-Nitropropane*. 1985.
41. Peter B. Mills, W.J.A., Francisco Prieto, John A. Alden, and Richard G. Compton*, *Heterogeneous ECE Processes at Channel Electrodes: Voltammetric Waveshape Theory. Application to the Reduction of Nitromethane at Platinum Electrodes*. J. Phys. Chem, 1998(102): p. 6573-6578.
42. Mansuy, D., J.C. Chottard, and G. Chottard, *Nitrosoalkanes as Fe(II) ligands in the hemoglobin and myoglobin complexes formed from nitroalkanes in reducing conditions*. Eur J Biochem, 1977. **76**(2): p. 617-23.
43. Guo, Z., et al., *Direct electrochemistry of hemoglobin and myoglobin at didodecyldimethylammonium bromide-modified powder microelectrode and application for electrochemical detection of nitric oxide*. Anal Chim Acta, 2008. **607**(1): p. 30-6.
44. Dai, Z., X. Xu, and H. Ju, *Direct electrochemistry and electrocatalysis of myoglobin immobilized on a hexagonal mesoporous silica matrix*. Anal Biochem, 2004. **332**(1): p. 23-31.
45. Bayachou, M. and J.A. Boutros, *Direct electron transfer to the oxygenase domain of neuronal nitric oxide synthase (NOS): exploring unique redox properties of NOS enzymes*. J Am Chem Soc, 2004. **126**(40): p. 12722-3.
46. Ling Li, M.B., *HEMOPROTEIN-MEDIATED ACTIVATION OF NITROALKANES*. 2009.
47. Ulman, A., *Formation and Structure of Self-Assembled Monolayers*. Chem Rev, 1996. **96**(4): p. 1533-1554.
48. Di Rocco, G., et al., *Axial iron coordination and spin state change in a heme c upon electrostatic protein-SAM interaction*. Phys Chem Chem Phys. **15**(32): p. 13499-505.
49. Ramsden, J.J., G.I. Bachmanova, and A.I. Archakov, *Immobilization of proteins to lipid bilayers*. Biosens Bioelectron, 1996. **11**(5): p. 523-8.
50. Danica Mimica a, Jose' H. Zagal b, Fethi Bedioui a,*, *Electroreduction of nitrite by hemin, myoglobin and hemoglobin in surfactant films*. Journal of Electroanalytical Chemistry, (2001). **497**: p. 106-113.
51. Prakash, P.A., U. Yogeswaran, and S.M. Chen, *A review on direct electrochemistry of catalase for electrochemical sensors*. Sensors (Basel), 2009. **9**(3): p. 1821-44.
52. Bayachou, M., L. Elkbir, and P.J. Farmer, *Catalytic two-electron reductions of N2O and N3- by myoglobin in surfactant films*. Inorg Chem, 2000. **39**(2): p. 289-93.
53. Hu, Y., N. Hu, and Y. Zeng, *Electrochemistry and electrocatalysis with myoglobin in biomembrane-like surfactant-polymer 2C12N+PA- composite films*. Talanta, 2000. **50**(6): p. 1183-95.
54. Dai, Z., et al., *Direct electrochemistry of myoglobin based on ionic liquid-clay composite films*. Biosens Bioelectron, 2009. **24**(6): p. 1629-34.
55. Kumar, S.A. and S.M. Chen, *Direct electrochemistry and electrocatalysis of myoglobin on redox-active self-assembling monolayers derived from nitroaniline modified electrode*. Biosens Bioelectron, 2007. **22**(12): p. 3042-50.
56. Groves, J.T. and C.C. Wang, *Nitric oxide synthase: models and mechanisms*. Curr Opin Chem Biol, 2000. **4**(6): p. 687-95.

57. Tejero, J., J. Santolini, and D.J. Stuehr, *Fast ferrous heme-NO oxidation in nitric oxide synthases*. FEBS J, 2009. **276**(16): p. 4505-14.
58. Fischmann TO, H.A., Niu XD, Fossetta JD, Lunn CA, Dolphin E, Prongay AJ, Reichert P, Lundell DJ, Narula SK, Weber PC., *Structural characterization of nitric oxide synthase isoforms reveals striking active-site conservation*. Nat Struct Biol., 1999. **6**(3): p. 233-242.
59. Mack Flinspach , H.L., Joumana Jamal ,Weiping Yang ,Hui Huang ,Richard B. Silverman, and Thomas L. Poulos, *Structures of the Neuronal and Endothelial Nitric Oxide Synthase Heme Domain with d-Nitroarginine-Containing Dipeptide Inhibitors Bound*. Biochemistry, 2004. **43**((18)): p. 5181–5187.
60. Robin J. Rosenfeld, E.D.G., Koustubh Panda, Gunilla Andersson, Anders Åberg, Alan V. Wallace, and A.J.O. Garrett M. Morris, Dennis J. Stuehr, John A. Tainer, and Elizabeth D. Getzoff, *Conformational Changes in Nitric Oxide Synthases Induced by Chlorzoxazone and Nitroindazoles: Crystallographic and Computational Analyses of Inhibitor Potency*. Biochemistry, 2002. **41**(47): p. 13915-13925.
61. Huiying Li , M.L.F., Jotaro Igarashi , Joumana Jamal , Weiping Yang , José Antonio Gómez-Vidal , Elizabeth A. Litzinger , Hui Huang , Erik P. Erdal , Richard B. Silverman , and Thomas L. Poulos *Exploring the Binding Conformations of Bulkier Dipeptide Amide Inhibitors in Constitutive Nitric Oxide Synthases*. Biochemistry, 2005. **44**(46): p. 15222–15229.
62. Salerno L, S.V., Di Giacomo C, Romeo G, Siracusa MA., *Progress in the development of selective nitric oxide synthase (NOS) inhibitors*. Curr Pharm Des., 2002. **8**(3): p. 177-200.
63. Roman Fedorov, E.H., Dipak K. Ghosh, and Ilme Schlichting, *Structural Basis for the Specificity of the Nitric-oxide Synthase Inhibitors W1400 and N-Propyl-L-Arg for the Inducible and Neuronal Isoforms*. J. Biol. Chem., 2003. **278**(46): p. 45818–45825.